NATIONAL ADVISORY COMMITTEE FOR AERONAUTICS

REPORT No. 723

WIND-TUNNEL INVESTIGATION OF NACA 23012, 23021 AND 23030 AIRFOILS EQUIPPED WITH 40-PERCENT-CHORD DOUBLE SLOTTED FLAPS

By THOMAS A. HARRIS and ISIDORE G. RECANT

1941

AERONAUTIC SYMBOLS

1. FUNDAMENTAL AND DERIVED UNITS

	Symbol	Metric		English	
		Unit	Abbreviation	Unit	Abbreviation
Length	l	meter	m	foot (or mile)	ft (or mi)
Time	t	second	s	second (or hour)	sec (or hr)
Force	F	weight of 1 kilogram	kg	weight of 1 pound	lb
Power	P	horsepower (metric)		horsepower	hp
Speed	V	kilometers per hour	kph	miles per hour	mph
		meters per second	mps	feet per second	fps

2. GENERAL SYMBOLS

W Weight$=mg$

g Standard acceleration of gravity$=9.80665$ m/s^2 or 32.1740 ft/sec^2

m Mass$=\frac{W}{g}$

I Moment of inertia$=mk^2$. (Indicate axis of radius of gyration k by proper subscript.)

μ Coefficient of viscosity

ν Kinematic viscosity

ρ Density (mass per unit volume)

Standard density of dry air, 0.12497 kg-m^{-4}-s^2 at 15° C and 760 mm; or 0.002378 lb-ft^{-4} sec^2

Specific weight of "standard" air, 1.2255 kg/m^3 or 0.07651 lb/cu ft

3. AERODYNAMIC SYMBOLS

S Area

S_w Area of wing

G Gap

b Span

c Chord

A Aspect ratio, $\frac{b^2}{S}$

V True air speed

q Dynamic pressure, $\frac{1}{2}\rho V^2$

L Lift, absolute coefficient $C_L=\frac{L}{qS}$

D Drag, absolute coefficient $C_D=\frac{D}{qS}$

D_0 Profile drag, absolute coefficient $C_{D_0}=\frac{D_0}{qS}$

D_i Induced drag, absolute coefficient $C_{D_i}=\frac{D_i}{qS}$

D_p Parasite drag, absolute coefficient $C_{D_p}=\frac{D_p}{qS}$

C Cross-wind force, absolute coefficient $C_C=\frac{C}{qS}$

i_w Angle of setting of wings (relative to thrust line)

i_t Angle of stabilizer setting (relative to thrust line)

Q Resultant moment

Ω Resultant angular velocity

R Reynolds number, $\rho\frac{Vl}{\mu}$ where l is a linear dimension (e.g., for an airfoil of 1.0 ft chord, 100 mph, standard pressure at 15° C, the corresponding Reynolds number is 935,400; or for an airfoil of 1.0 m chord, 100 mps, the corresponding Reynolds number is 6,865,000)

α Angle of attack

ϵ Angle of downwash

α_0 Angle of attack, infinite aspect ratio

α_i Angle of attack, induced

α_a Angle of attack, absolute (measured from zero-lift position)

γ Flight-path angle

I

REPORT No. 723

WIND-TUNNEL INVESTIGATION OF NACA 23012, 23021 AND 23030 AIRFOILS EQUIPPED WITH 40-PERCENT-CHORD DOUBLE SLOTTED FLAPS

By THOMAS A. HARRIS and ISIDORE G. RECANT
Langley Memorial Aeronautical Laboratory

I -a

NATIONAL ADVISORY COMMITTEE FOR AERONAUTICS

HEADQUARTERS, NAVY BUILDING, WASHINGTON, D. C.

Created by act of Congress approved March 3, 1915, for the supervision and direction of the scientific study of the problems of flight (U. S. Code, Title 50, Sec. 151). Its membership was increased to 15 by act approved March 2, 1929. The members are appointed by the President, and serve as such without compensation.

TECHNICAL COMMITTEES

AERODYNAMICS
POWER PLANTS FOR AIRCRAFT
AIRCRAFT MATERIALS

AIRCRAFT STRUCTURES
AIRCRAFT ACCIDENTS
INVENTIONS AND DESIGNS

Coordination of Research Needs of Military and Civil Aviation

Preparation of Research Programs

Allocation of Problems

Prevention of Duplication

Consideration of Inventions

LANGLEY MEMORIAL AERONAUTICAL LABORATORY

LANGLEY FIELD, VA.

AMES AERONAUTICAL LABORATORY

MOFFETT FIELD, CALIF.

Conduct, under unified control, for all agencies, of scientific research on the fundamental problems of flight.

OFFICE OF AERONAUTICAL INTELLIGENCE

WASHINGTON. D. C.

Collection, classification, compilation, and dissemination of scientific and technical information on aeronautics

NATIONAL ADVISORY COMMITTEE FOR AERONAUTICS

HEADQUARTERS, NAVY BUILDING, WASHINGTON, D. C.

Created by act of Congress approved March 3, 1915, for the supervision and direction of the scientific study of the problems of flight (U. S. Code, Title 50, Sec. 151). Its membership was increased to 15 by act approved March 2, 1929. The members are appointed by the President, and serve as such without compensation.

TECHNICAL COMMITTEES

AERODYNAMICS
POWER PLANTS FOR AIRCRAFT
AIRCRAFT MATERIALS

AIRCRAFT STRUCTURES
AIRCRAFT ACCIDENTS
INVENTIONS AND DESIGNS

Coordination of Research Needs of Military and Civil Aviation

Preparation of Research Programs

Allocation of Problems

Prevention of Duplication

Consideration of Inventions

LANGLEY MEMORIAL AERONAUTICAL LABORATORY

LANGLEY FIELD, VA.

AMES AERONAUTICAL LABORATORY

MOFFETT FIELD, CALIF.

Conduct, under unified control, for all agencies, of scientific research on the fundamental problems of flight.

OFFICE OF AERONAUTICAL INTELLIGENCE

WASHINGTON. D. C.

Collection, classification, compilation, and dissemination of scientific and technical information on aeronautics

REPORT No. 723

WIND-TUNNEL INVESTIGATION OF NACA 23012, 23021, AND 23030 AIRFOILS EQUIPPED WITH 40-PERCENT-CHORD DOUBLE SLOTTED FLAPS

By Thomas A. Harris and Isadore G. Recant

SUMMARY

An investigation was conducted in the NACA 7- by 10-foot wind tunnel to determine the effect of the deflection of main and auxiliary slotted flaps on the aerodynamic section characteristics of large-chord NACA 23012, 23021, and 23030 airfoils equipped with 40-percent-chord double slotted flaps. The complete aerodynamic section characteristics and envelope polar curves are given for each airfoil-flap combination. The effect of airfoil-thickness is shown, and comparisons are made of single slotted flaps with double slotted flaps on each of the airfoils.

The maximum section lift coefficient of an airfoil with a 40-percent-chord double slotted flap was found to increase slowly with increasing thickness, reaching a value of 3.7 for the 30-percent-thick airfoil. For any airfoil thickness, the double slotted flap gave a higher value of section maximum lift coefficient than either the 40-percent-chord or the 25.66-percent-chord single slotted flaps. The large lift coefficients for the double slotted flaps were accompanied by large pitching-moment coefficients. The section profile-drag coefficient of an airfoil with a double slotted flap increased with an increase in thickness at all except very high lift coefficients. For a given airfoil thickness, the double and the single slotted flaps gave about the same section profile-drag coefficients for section lift coefficients less than 2.0; above this value the double slotted flap gave the lower section profile-drag coefficients.

INTRODUCTION

The National Advisory Committee for Aeronautics has undertaken an extensive investigation of various airfoil-flap combinations to furnish information applicable to the aerodynamic design of high-lift devices for improving the safety and the performance of airplanes. A high-lift device capable of producing high lift with variable drag for landing and high lift with low drag for take-off and initial climb is believed to be desirable. Other desirable aerodynamic features are no increase in drag with the flap neutral; small change in pitching moment with flap deflection; low forces required to operate the flap; and freedom from possible hazard due to icing.

The results of an investigation of a 25-percent-chord single-slotted flap on airfoils of 12-, 21-, and 30-percent thickness are reported in references 1 to 3; results of a 40-percent-chord single-slotted flap on the same airfoils are reported in references 3, 4, and 5. The Fowler and the venetian-blind flaps have also been investigated on the 12-percent-thick airfoil, and the results are reported in references 1 and 6. Data are presented in reference 7 for split flaps of various chord on 12-, 21-, and 30-percent-thick airfoils. The results of tests of a 25-percent-chord double-slotted flap on the 12-percent thick airfoil are reported in reference 8.

The data presented in reference 8 indicated that the double slotted flap was superior to the single slotted flap for high lift and for low drag at the high section lift coefficients. In the present report are given the results of the tests of the NACA 23012, 23021, and 23030 airfoils, each equipped with a 40-percent-chord double slotted flap.

MODELS

PLAIN AIRFOILS

Three basic models, or plain airfoils, were used in these tests; each had a chord of 3 feet and a span of 7 feet. The models were constructed of laminated wood and were built to the NACA 23012, 23021, and 23030 profiles. The thickness of each of these airfoils is, respectively, 12, 21, and 30 percent of the airfoil chord. The airfoil ordinates are given in table I. These airfoils had previously been used for the split-flap investigation reported in reference 7.

SLOTTED FLAPS

Slot shapes.—The slot shapes used were the same as those used for the single slotted flaps reported in references 1 to 5. The piece forming the slot shape for the main slotted flap was attached directly to the main portion of the airfoil; for the auxiliary flap the slot shape was formed by cutting the trailing edge of the main flap. The slot shapes for the three airfoils are shown in figure 1.

Flaps.—The flap contours were the same as those used in the investigation of the single slotted flaps reported in references 1 to 5. The main flap was hinged to the main portion of the airfoil by special fittings, and the auxiliary flap was hinged to the main flap. The flap shapes are shown in figure 1 and the flap ordinates are given in table II. The deflection of the main flap is measured between the flap chord and the chord of the

main airfoil; whereas, for the auxiliary flap the deflection is measured between its chord and the chord of the main flap.

The models were made to a tolerance of ±0.015 inch.

TESTS

The models were mounted vertically in the closed test section of the NACA 7- by 10-foot wind tunnel so as to span the jet completely except for small clearances at each end. (See references 1 and 9.) The main airfoil was rigidly attached to the balance frame by torque

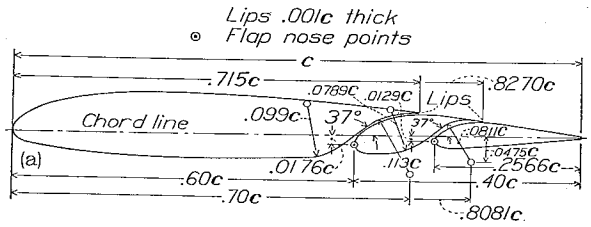

(a) NACA 23012 airfoil with double slotted flap.

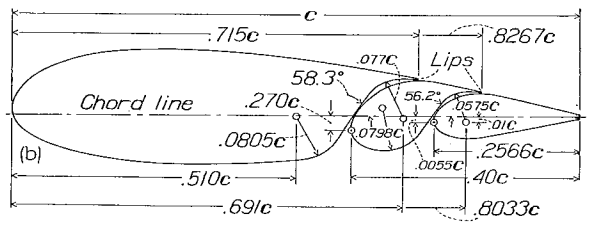

(b) NACA 23021 airfoil with double slotted flap.

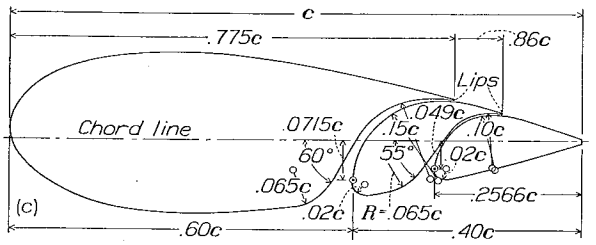

(c) NACA 23030 airfoil with double slotted flap.

FIGURE 1.—Sections of NACA 23012, 23021, and 23030 airfoils with 40 percent-chord double slotted flaps.

tubes, which extended through the upper and the lower boundaries of the tunnel. The angle of attack of the model was set from outside the tunnel by rotating the torque tubes with a calibrated electric drive. Approximately two-dimensional flow is obtained with this type of installation and the aerodynamic section characteristics of the model under test can be determined.

A dynamic pressure of 16.37 pounds per square foot was maintained for all the tests, which corresponds to a velocity of about 80 miles per hour under standard atmospheric conditions and to an average test Reynolds number of about 2,190,000. Because of the turbulence in the wind tunnel, the effective Reynolds number R_e was approximately 3,500,000. (See reference 10.) For all tests, R_e is based on the chord of the airfoil with the flap retracted and on a turbulence factor of 1.6 for the tunnel.

No tests were made of the plain airfoils because they were the same airfoils used in the investigation of the split flaps reported in reference 7. Tests were made, however, to determine the effects of the breaks in the surface of the airfoil with the flaps undeflected.

Because of the large number of tests involved in determining the optimum paths for the main and the auxiliary flaps on each airfoil, it was assumed that the optimum paths for the single slotted flaps (references 1 to 5) would be the optimum paths for the combination. Tests were therefore made for each position and deflection of the main flap as previously determined. For each position and deflection of the main flap, the auxiliary flap was tested at its previously determined optimum positions and deflections. For each airfoil-flap combination, the flaps were deflected through a sufficient range to obtain the maximum lift coefficient.

An angle-of-attack range from −6° to the angle of attack for maximum lift was covered in 2° increments for each test. Lift, drag, and pitching moment were measured at each angle of attack.

RESULTS AND DISCUSSION

COEFFICIENTS

All test results are given in standard section nondimensional coefficient form corrected for tunnel-wall effect and turbulence as explained in reference 1.

c_l	section lift coefficient (l/qc)
c_{d_0}	section profile-drag coefficient (d_0/qc)
$c_{m_{(a.c.)_0}}$	section pitching-moment coefficient about aerodynamic center of plain airfoil ($m_{(a.c.)_0}/qc^2$)
$c_{l_{e_{max}}}$	section effective maximum lift coefficient $\left(c_{l_{max}}+\frac{\left[c_{m_{(a.c.)_0}}\right]_{c_{l_{max}}}}{l_t}\right)$

where

l	section lift
d_0	section profile drag
$m_{(a.c.)_0}$	section pitching moment
q	dynamic pressure ($1/2\rho V^2$)
c	chord of basic airfoil with flap fully retracted
$c_{l_{max}}$	section maximum lift coefficient
$\left[c_{m(a.c.)_0}\right]_{c_{l_{max}}}$	section pitching-moment coefficient at maximum lift coefficient
l_t	distance from aerodynamic center of airfoil to center of pressure of tail, expressed in airfoil chords

and

α_0 angle of attack for infinite aspect ratio

δ_{f_1} main flap deflection

δ_{f_2} auxiliary flap deflection

PRECISION

The accuracy of the various measurements in the tests is believed to be within the following limits:

α_0	±0.1°	$c_{d_{0(c_l=1.0)}}$	±0.0006
$c_{l_{max}}$	±0.03	$c_{d_{0(c_l=2.5)}}$	±0.002
$c_{m_{(a.c.)_0}}$	±0.003	δ_{f_1} and δ_{f_2}	±0.2°
$c_{d_{0_{min}}}$	±0.0003	Flap position	±0.001c

The data from the tests with the main and the auxiliary flaps retracted and undeflected have been corrected both for the effect of breaks in the surface at the slot entries and exits and for the effect of the flap hinges. No such corrections were applied when the flaps were deflected because of the large number of tests required, but it is believed that the relative merits of the various arrangements are inappreciably affected.

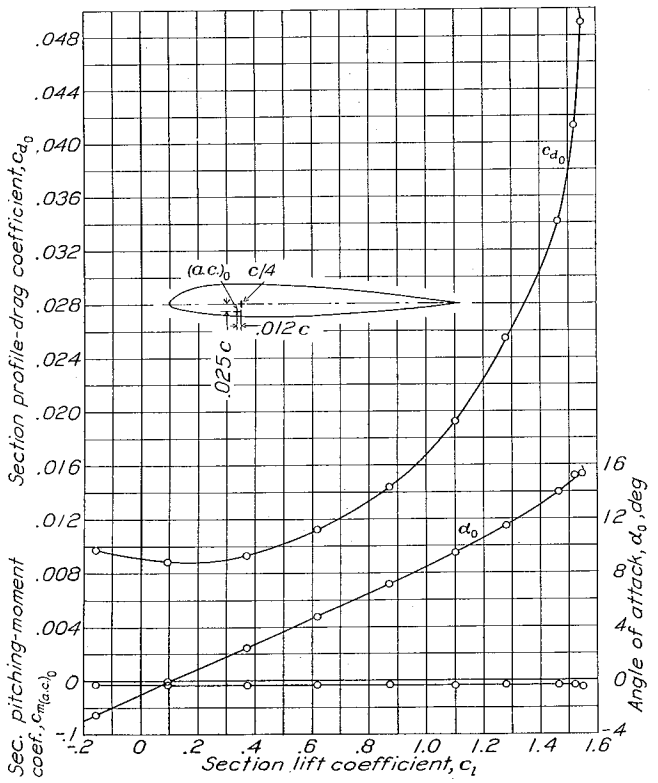

FIGURE 2.—Aerodynamic section characteristics of NACA 23012 plain airfoil.

AERODYNAMIC SECTION CHARACTERISTICS

Plain airfoils.—The complete aerodynamic section characteristics of the three basic airfoils tested are given in figures 2, 3, and 4. Because these data have already been discussed in reference 7, no further comment is believed necessary.

Effect of breaks in surface.—The effect on the section profile-drag coefficient of the breaks in the airfoil surfaces at the slot entries and exits when the flaps are retracted is shown in figure 5. In these tests the slots were sealed so that there was no air flow through them. The breaks in the surface of the NACA 23012 airfoil cause an increase in the section profile-drag coefficient from 0.003 to 0.004 throughout the lift range. For the NACA 23021 airfoil, the increment of the section profile-drag coefficient is 0.0055 at a section lift coefficient of 0, increases to 0.0072 at c_l=0.75, and then decreases to 0.0048 at c_l=1.2. For the NACA 23030 airfoil, the increment of the section profile-drag coefficient decreases from about 0.012 at low section lift coefficients to about 0.008 at c_l=0.8. With properly designed doors and flaps to close the breaks in the lower surface of the airfoils, all or most of the drag increment may be eliminated.

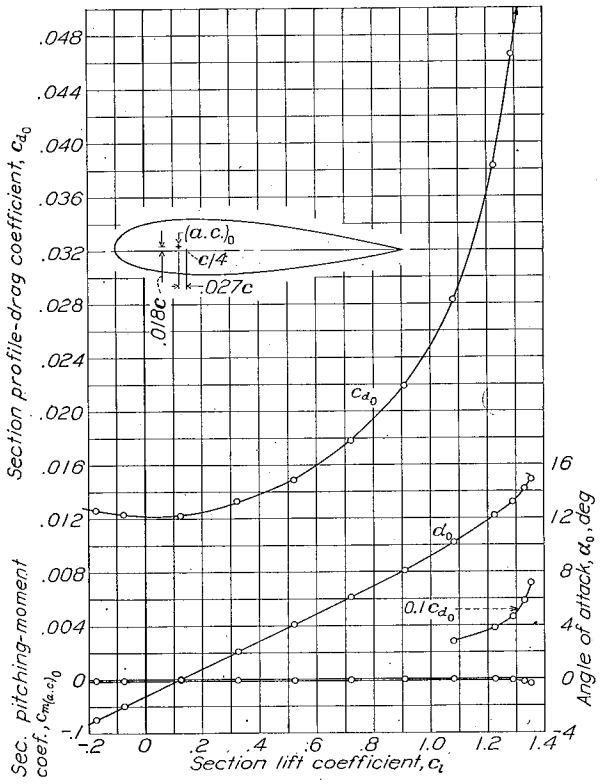

FIGURE 3.—Aerodynamic section characteristics of NACA 23021 plain airfoil.

Airfoils with double slotted flaps.—The aerodynamic section characteristics of the airfoils tested with 40-percent double slotted flaps are presented in figures 6 to 10 for the NACA 23012 airfoil, in figures 11 to 15 for the NACA 23021 airfoil, and in figures 16 to 20 for the NACA 23030 airfoil. These figures show the effect of variation of auxiliary flap deflection δ_{f_2} for a given

main flap deflection δ_{f_1}. As has been previously pointed out, a complete investigation of all the combinations of flap deflection and position for the main and the auxiliary flaps on each airfoil would require a prohibitive number of tests. It was therefore decided to move and to deflect the main and the auxiliary flaps of each airfoil along the optimum paths determined in previous tests of each flap as a single slotted flap. The following table gives the source from which each flap path was obtained.

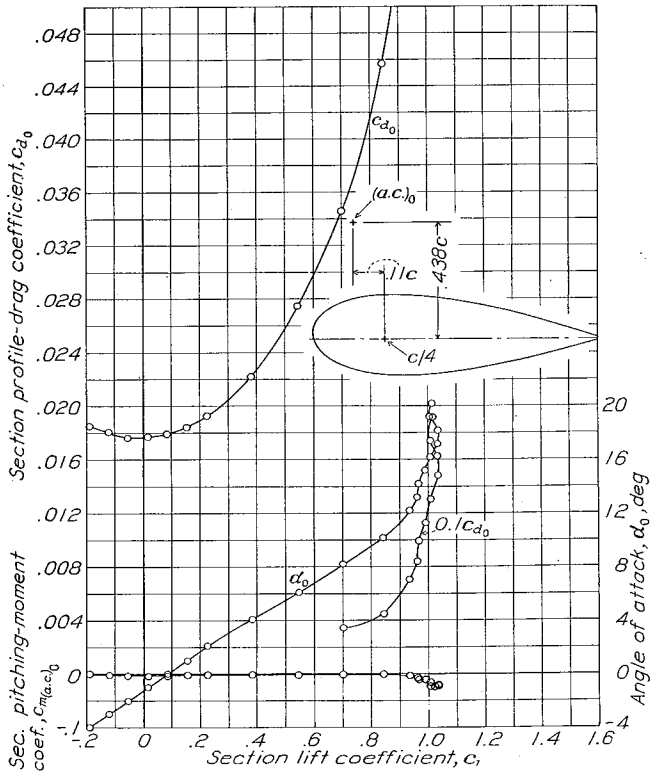

FIGURE 4.—Aerodynamic section characteristics of NACA 23030 plain airfoil.

NACA airfoil	Flap	Flap designation in reference	Reference
23012	Main	0.40c flap 1–b	4
	Auxiliary	0.2566c flap 2–h	1
23021	Main	0.40c flap 1–b	5
	Auxiliary	0.2566c flap 2–b	2
23030	Main	0.40c flap 1–b	3
	Auxiliary	0.2566c flap 1–b	3

The path of the auxiliary flap on the NACA 23012 airfoil is the optimum indicated by reference 1 only for a main flap deflection of 0°. For other values of δ_{f_1}, the auxiliary flap was moved along a path as close to the optimum as the hinge fittings permitted. This procedure was necessitated by the fact that the fittings had been altered after the single slotted flap had been tested. In any case, the actual paths followed by the flaps are shown on the figures.

Inspection of figures 6 to 20 shows that deflection of either auxiliary or main flaps affects the slopes of the lift curves to some degree, which is determined by the flap deflection and the airfoil thickness. Any deflection of the auxiliary flap, in general, increases the slope of the lift curve over that of the plain airfoil. This effect is apparently a function of airfoil thickness, the increase in slope being about 5 percent, 13 percent, and 60 percent for the NACA 23012, 23021, and 23030 airfoils, respectively. (See figs. 6, 11, and 16.) It may be noted, however, that the slopes of the lift curves for the three airfoils with the auxiliary flaps deflected are about the same. Deflection of the main flaps for all but the 30-percent-thick airfoil tends to decrease the lift-curve slope although the slope still remains higher than for the plain airfoils.

At a given section lift coefficient and main flap deflection, the negative pitching-moment coefficient increases with auxiliary flap deflection for all the airfoils. The section pitching-moment coefficient also increases rapidly with main flap deflection. The change in slope of the pitching-moment curves for large flap deflections may be undesirable. It should be noted, however, that the destablizing effect at these large flap deflections and high lift coefficients is not very pronounced for flap deflections below the optimum for maximum lift coefficients, except for the 30-percent-thick airfoil.

Polar envelope curves for each main flap deflection, obtained from figures 6 to 20, are plotted in figures 21, 22, and 23 for the NACA 23012, 23021, and 23030 airfoils, respectively. These polars show the lowest section profile-drag coefficient obtainable at a given section lift coefficient for a constant main flap deflection.

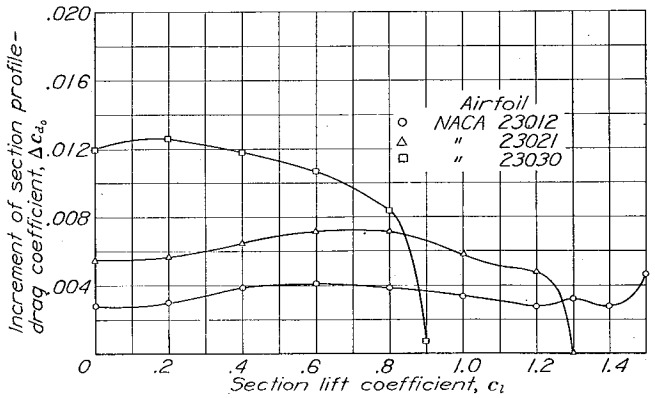

FIGURE 5.—Increment of section profile-drag coefficient due to breaks in the surfaces of the airfoils at the slot entrances and exits for the NACA 230 series with 0.40c double slotted flaps. $\delta_{f_1}=\delta_{f_2}=0$.

In the case of the NACA 23012 airfoil (fig. 21) it is shown that, for section lift coefficients less than 1.2, the plain airfoil gives the lowest section profile-drag coefficients. At higher section lift coefficients, a main flap deflection of 30° gives the lowest section profile-drag coefficient. In reference 4 it is pointed out that the drag for $\delta_{f_1}=30°$ at $\delta_{f_2}=0°$ is erratic, and it is believed that the values of c_{d_0} over the lift range from $c_l=1.4$ to $c_l=1.9$ should be disregarded. The 30° deflection is optimum for maximum section lift coefficient.

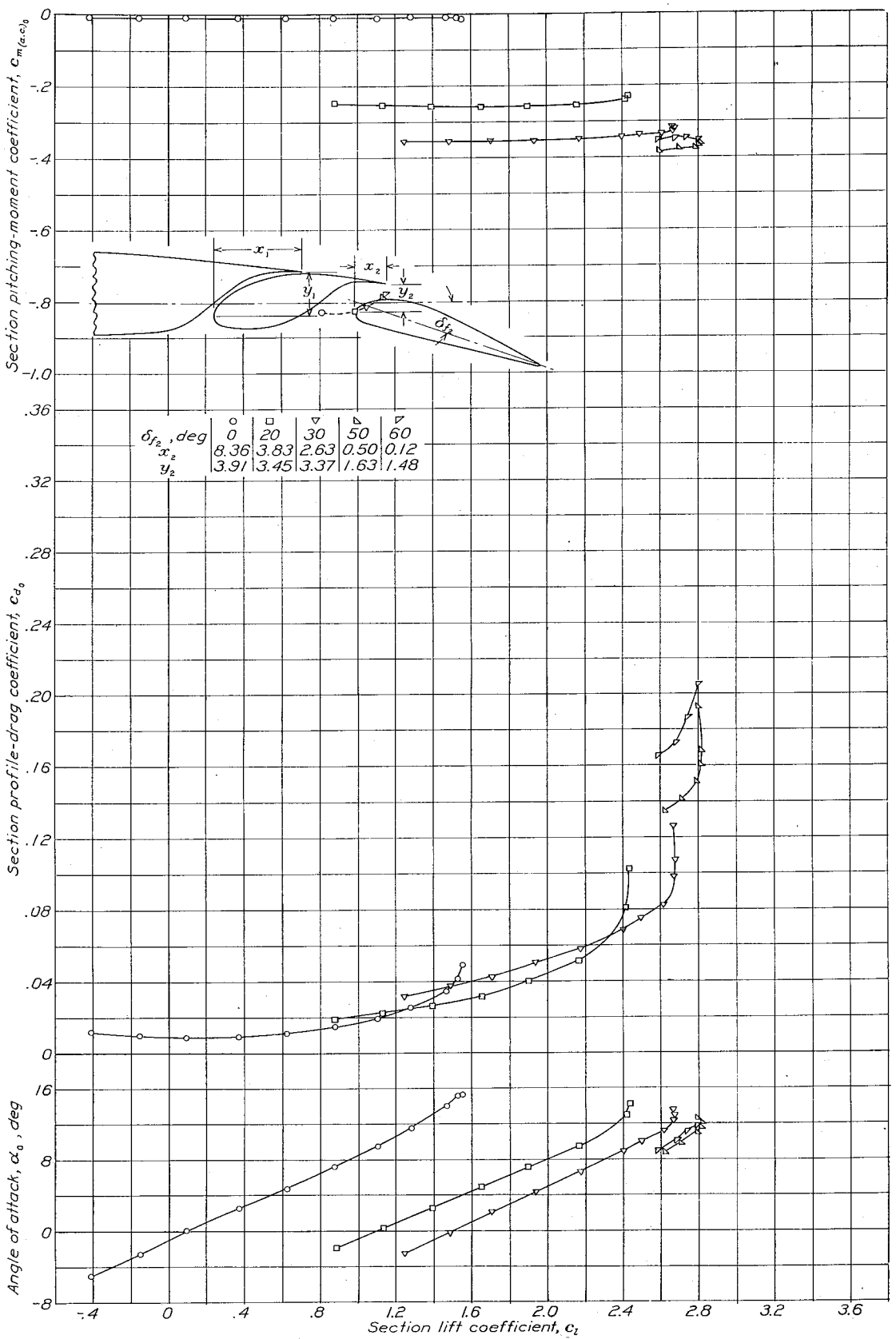

FIGURE 6.—Aerodynamic section characteristics of NACA 23012 airfoil with 40-percent-chord double slotted flap. $\delta_{f1}=0°$; $x_1=11.50$; $y_1=5.86$. x_1, y_1, x_2, y_2 are given in percent airfoil chord.

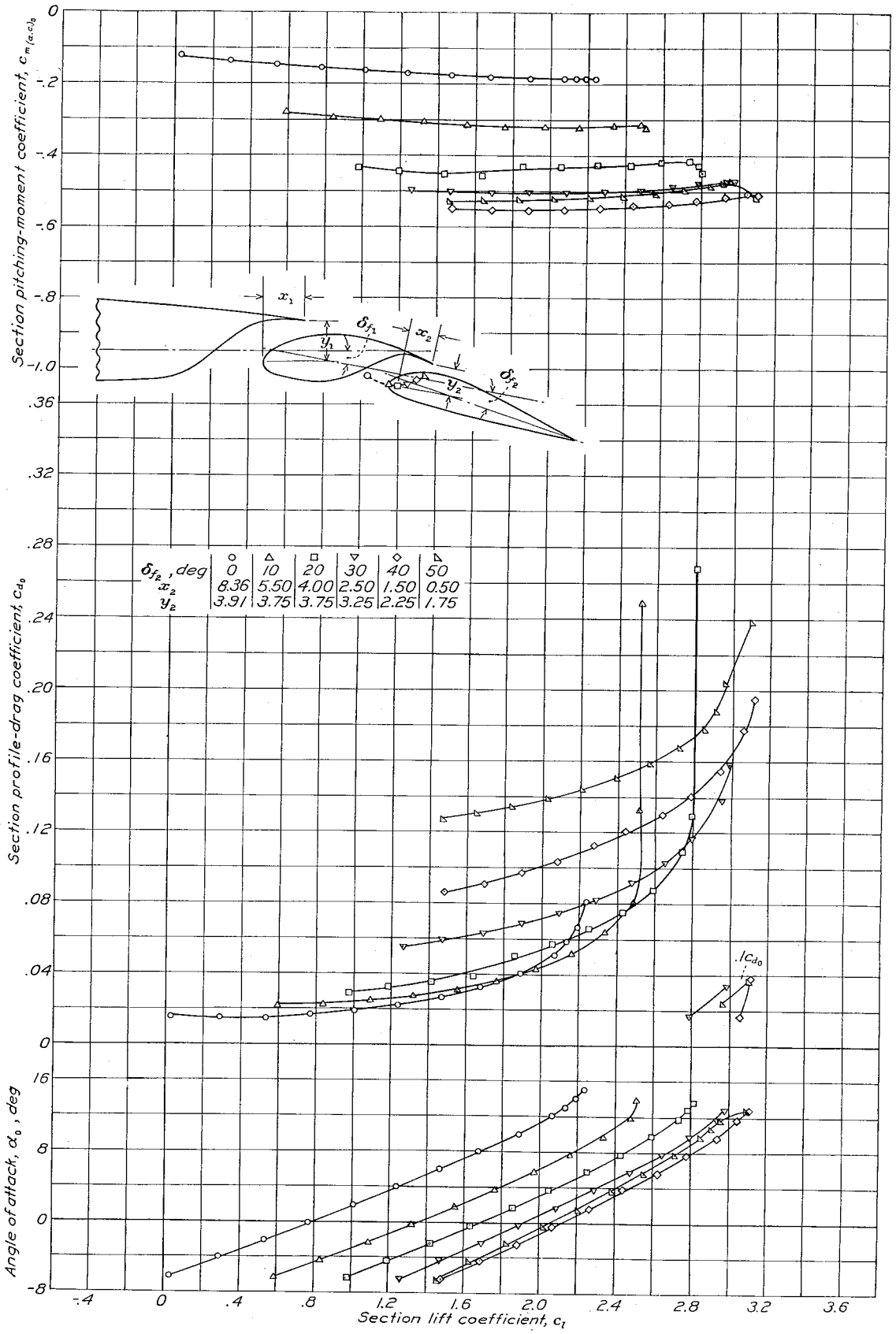

FIGURE 7.—Aerodynamic section characteristics of NACA 23012 airfoil with 40-percent-chord double slotted flap. $\delta_{f_1}=10°$; $x_1=5.50$; $y_1=5.50$. x_1, y_1, x_2, y_2 are given in percent airfoil chord.

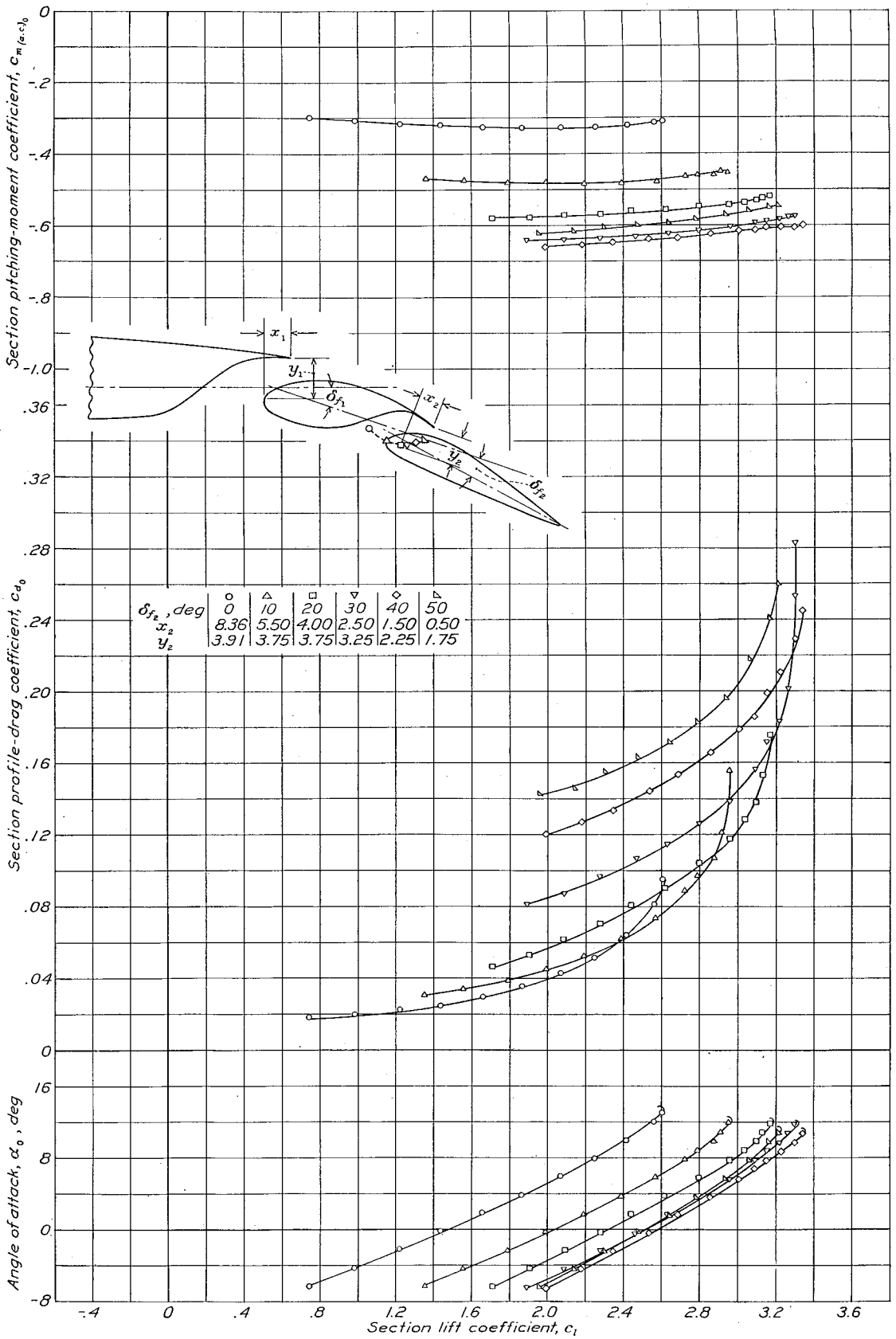

FIGURE 8.—Aerodynamic section characteristics of NACA 23012 airfoil with 40-percent-chord double slotted flap. δ_{f_1}=20°; x_1=3.50; y_1=5.50; x_1, y_1, x_2, y_2 are given in percent airfoil chord.

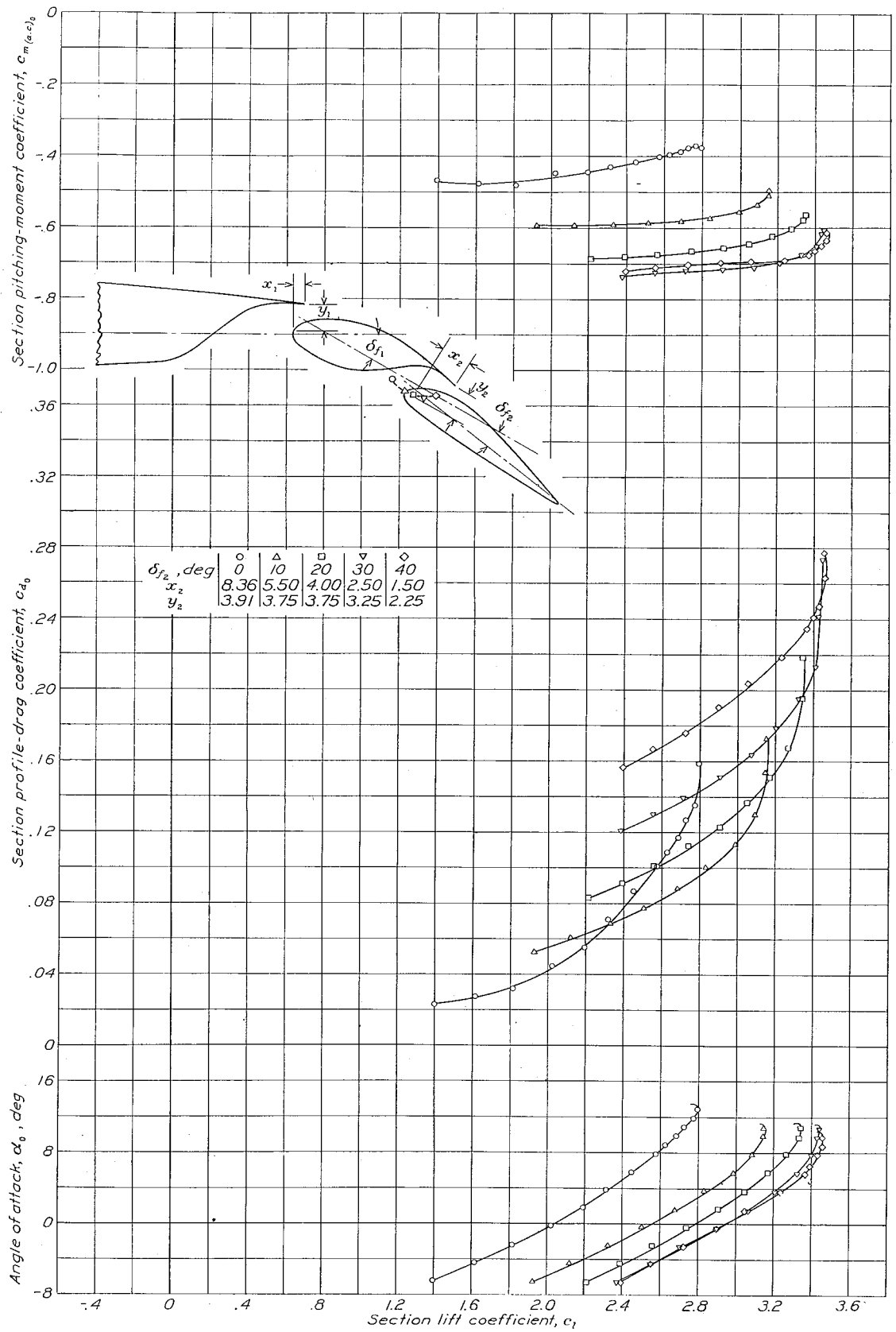

FIGURE 9.—Aerodynamic section characteristics of NACA 23012 airfoil with 40-percent-chord double slotted flap. $\delta_{f_1}=30°$; $x_1=1.50$; $y_1=3.50$. x_1, y_1, x_2, y_2 are given in percent airfoil chord.

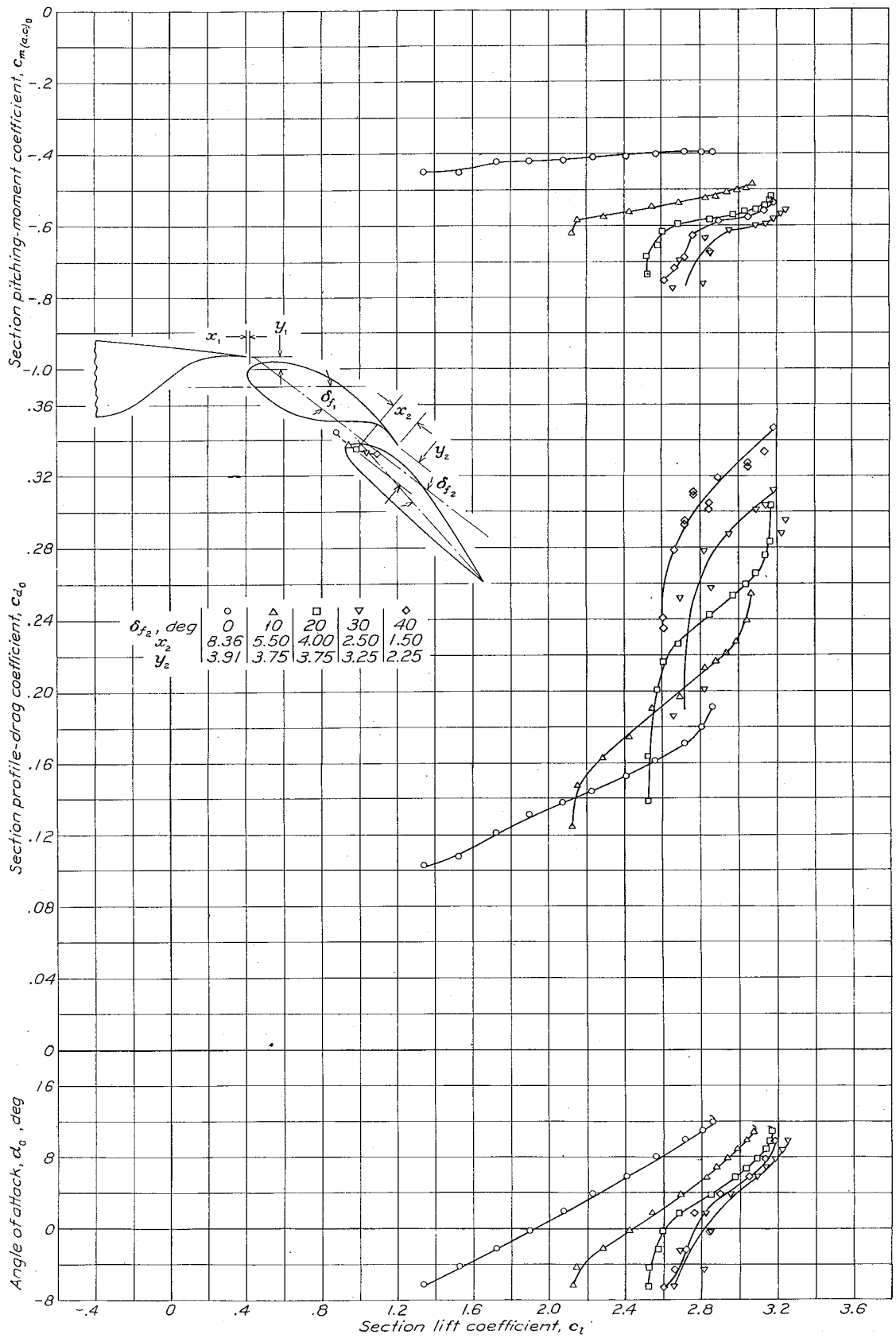

FIGURE 10.—Aerodynamic section characteristics of NACA 23012 airfoil with 40-percent-chord double slotted flap. $\delta_{f_1}=40°$; $x_1=-0.50$; $y_1=1.50$. x_1, y_1, x_2, y_2 are given in percent airfoil chord.

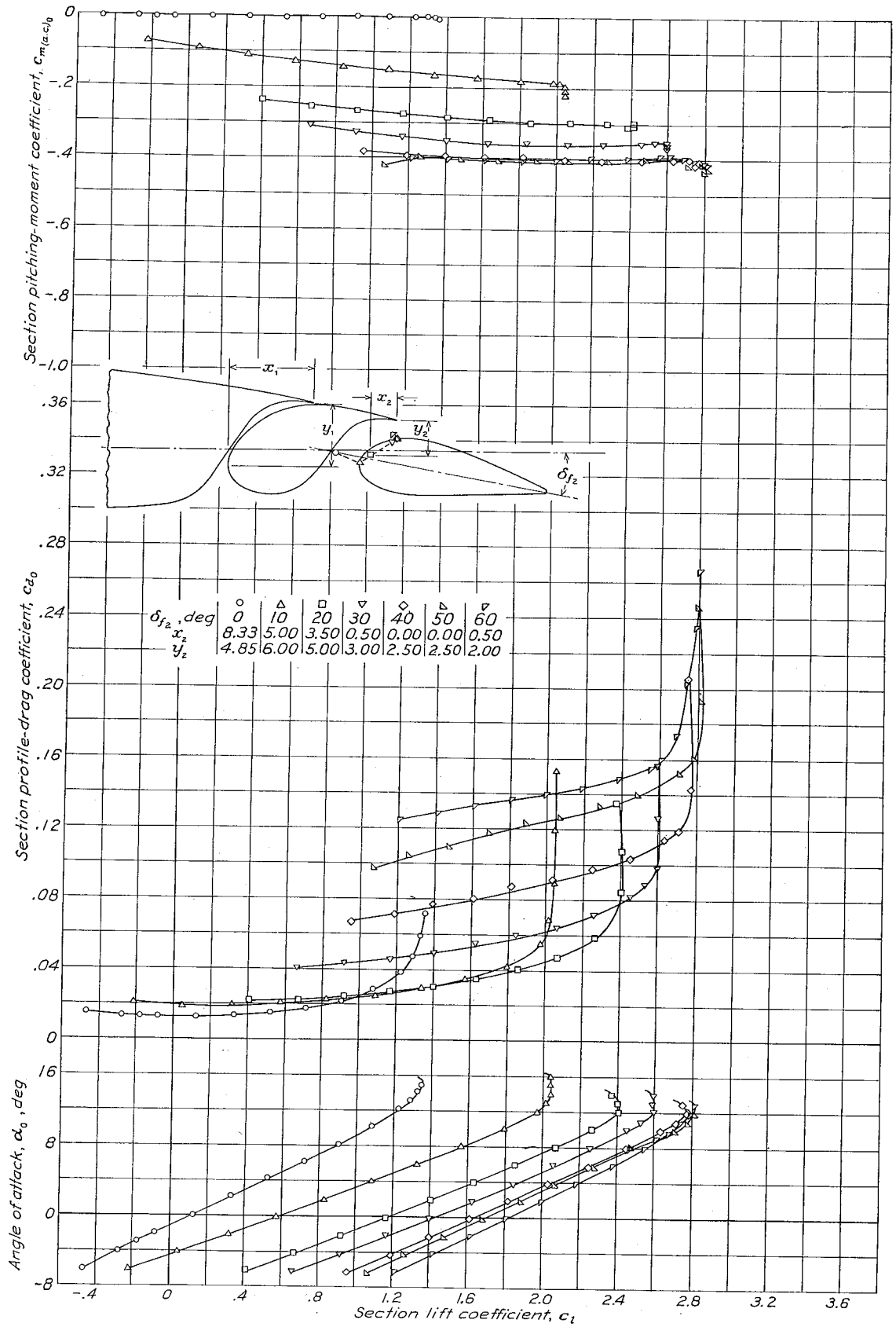

FIGURE 11.—Aerodynamic section characteristics of NACA 23021 airfoil with 40-percent-chord double slotted flap. $\delta_{f_1}=0°$; $x_1=11.50$; $y_1=9.20$. x_1, y_1, x_2, y_2 are given in percent airfoil chord.

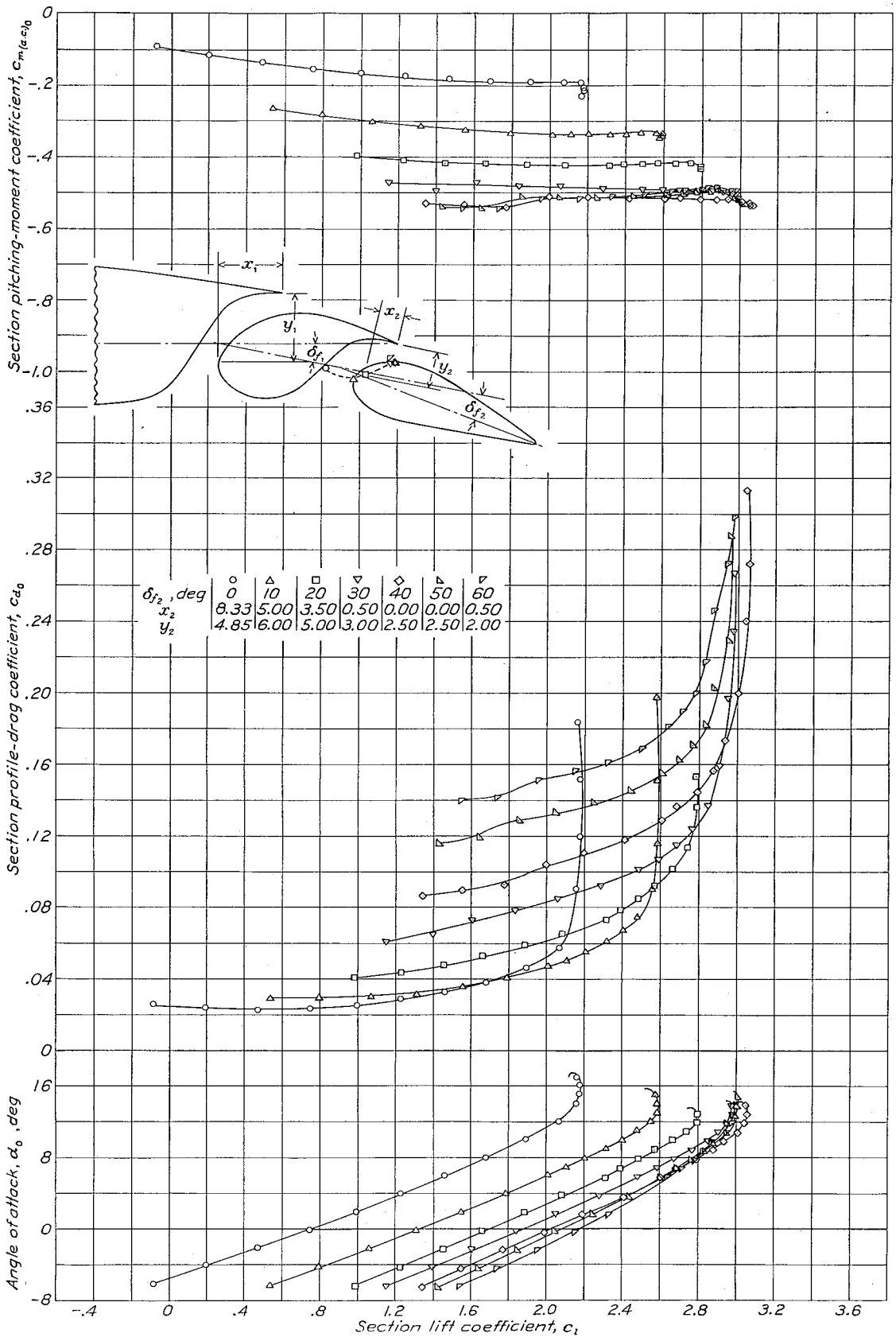

FIGURE 12.—Aerodynamic section characteristics of NACA 23021 airfoil with 40-percent-chord double slotted flap. $\delta_{f_1}=10°$; $x_1=8.50$; $y_1=9.50$. x_1, y_1, x_2, y_2 are given in percent airfoil chord.

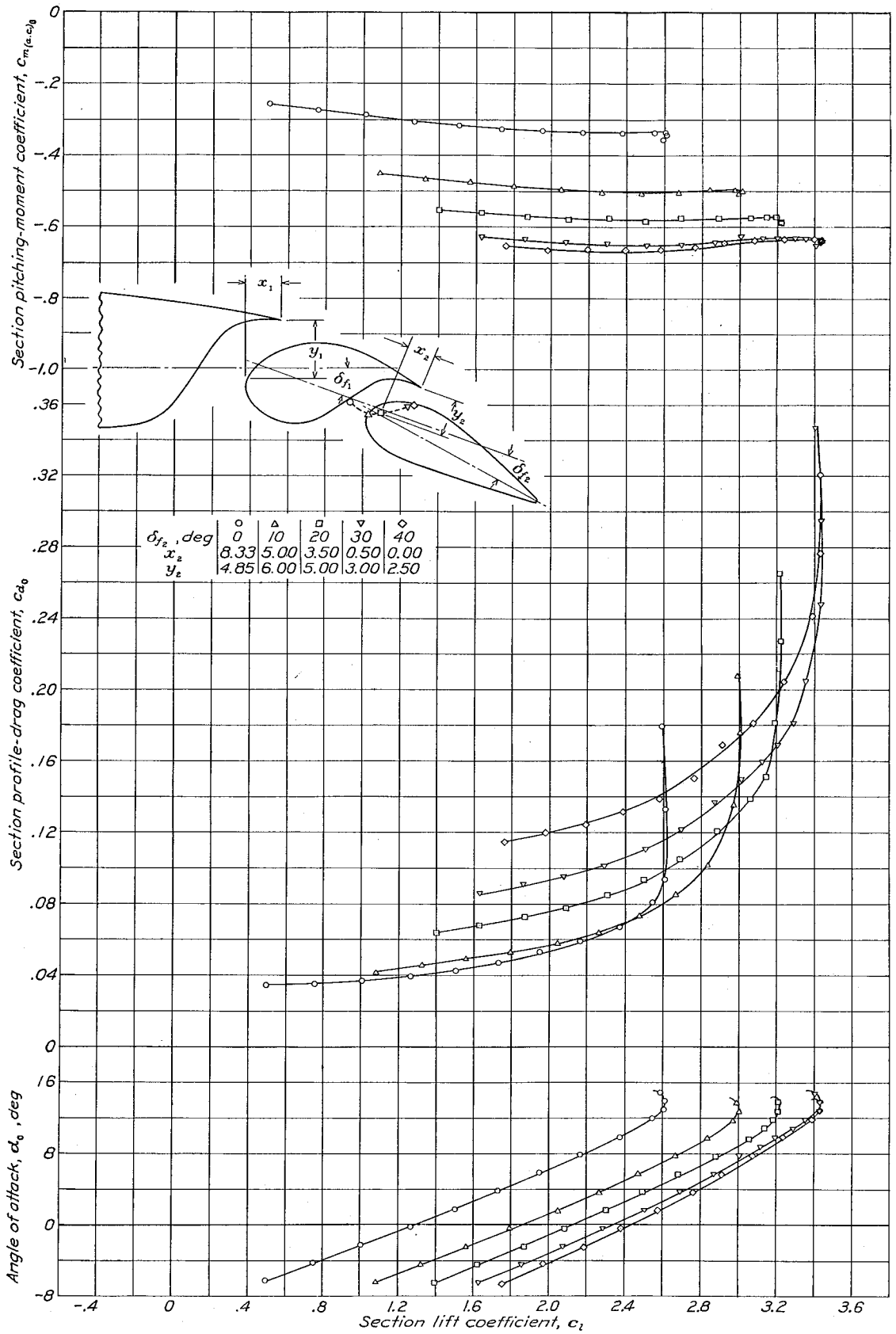

FIGURE 13.—Aerodynamic section characteristics of NACA 23021 airfoil with 40-percent-chord double slotted flap. $\delta_{f1}=20°$; $x_1=4.50$; $y_1=8.50$. x_1, y_1, x_2, y_2 are given in percent airfoil chord.

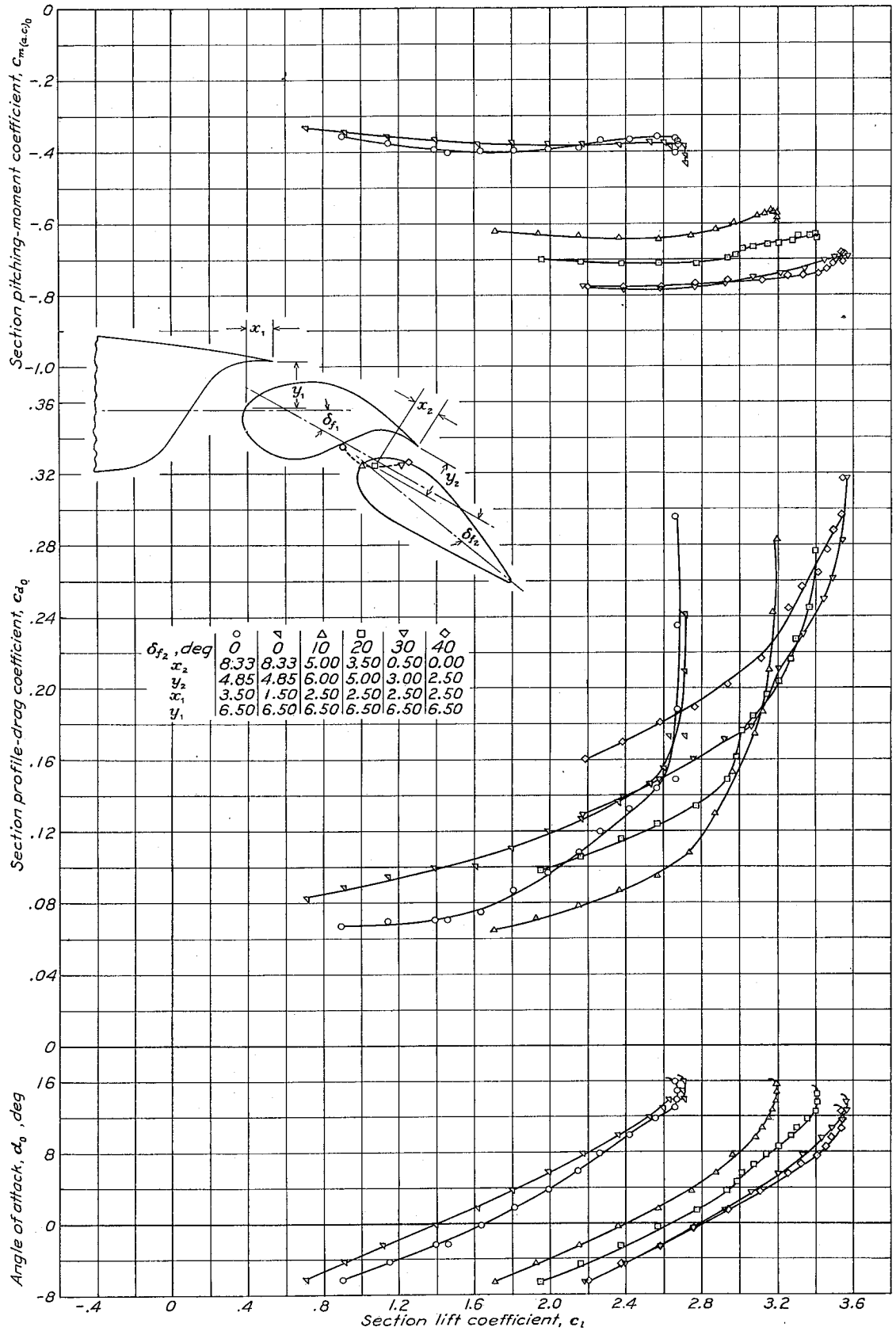

δ_{f_2}, deg	○ 0	◁ 0	△ 10	□ 20	▽ 30	◇ 40
x_2	8.33	8.33	5.00	3.50	0.50	0.00
y_2	4.85	4.85	6.00	5.00	3.00	2.50
x_1	3.50	1.50	2.50	2.50	2.50	2.50
y_1	6.50	6.50	6.50	6.50	6.50	6.50

FIGURE 14.—Aerodynamic section characteristics of NACA 23021 airfoil with 40-percent-chord double slotted flap. $\delta_{f_1}=30°$. x_1, y_1, x_2, y_2 are given in percent airfoil chord.

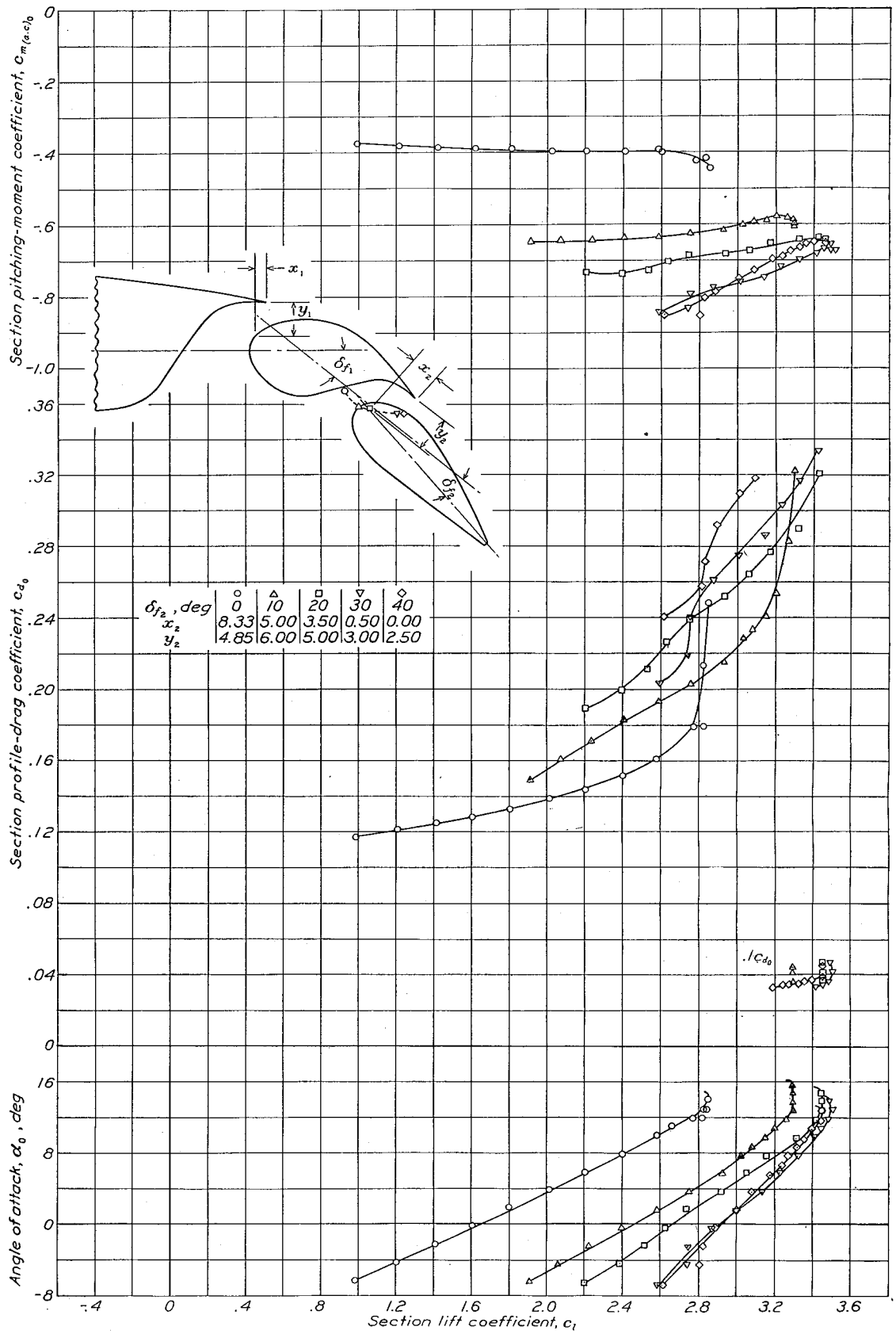

FIGURE 15.—Aerodynamic section characteristics of NACA 23021 airfoil with 40-percent-chord double slotted flap. $\delta_{f_1}=40°$; $x_1=1.50$; $y_1=4.50$. x_1, y_1, x_2, y_2 are given in percent airfoil chord.

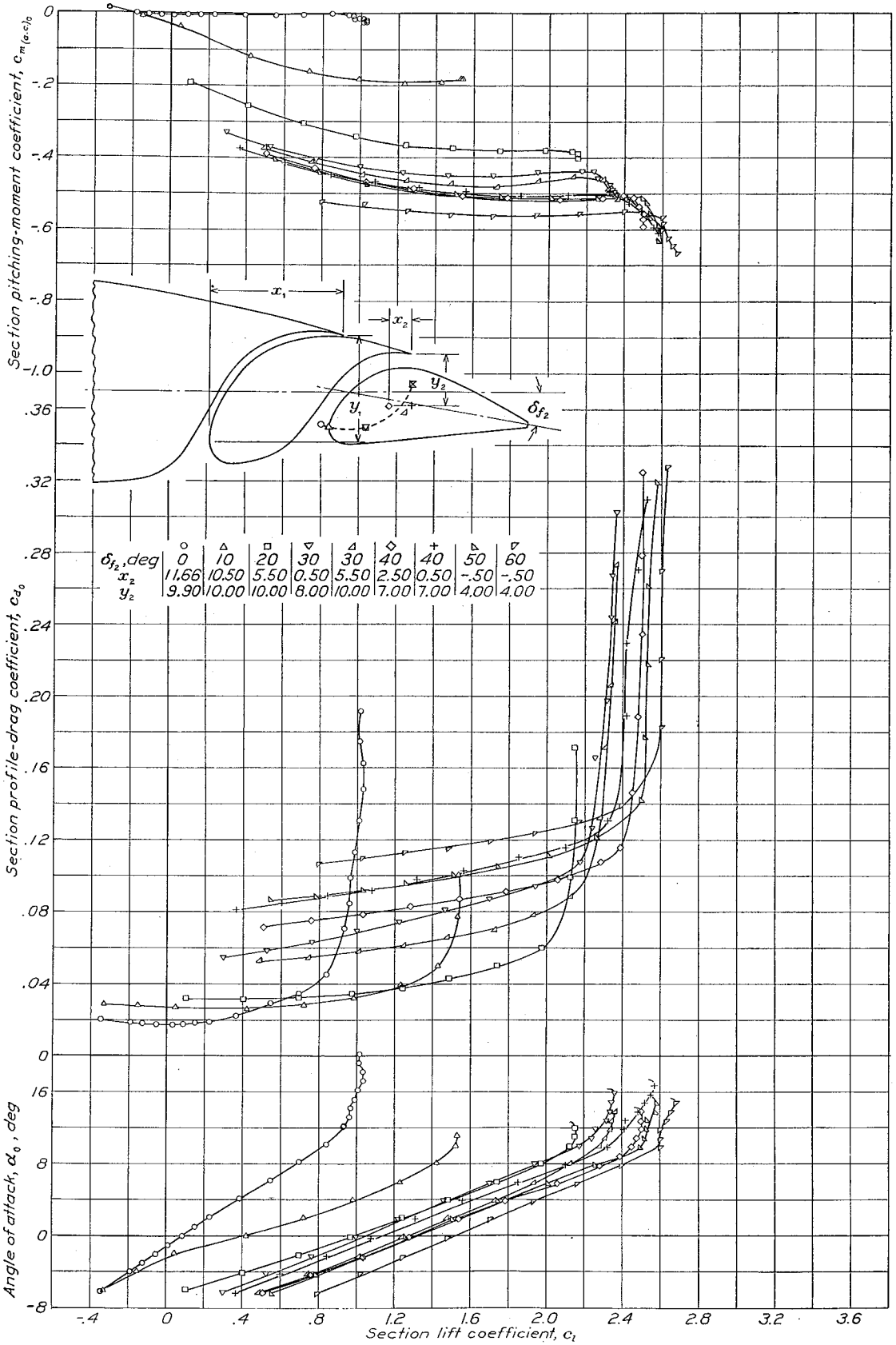

FIGURE 16.—Aerodynamic section characteristics of NACA 23030 airfoil with 40-percent-chord double slotted flap. $\delta_{f_1}=0°$; $x_1=17.00$; $y_1=14.85$. x_1, y_1, x_2, y_2 are given in percent airfoil chord.

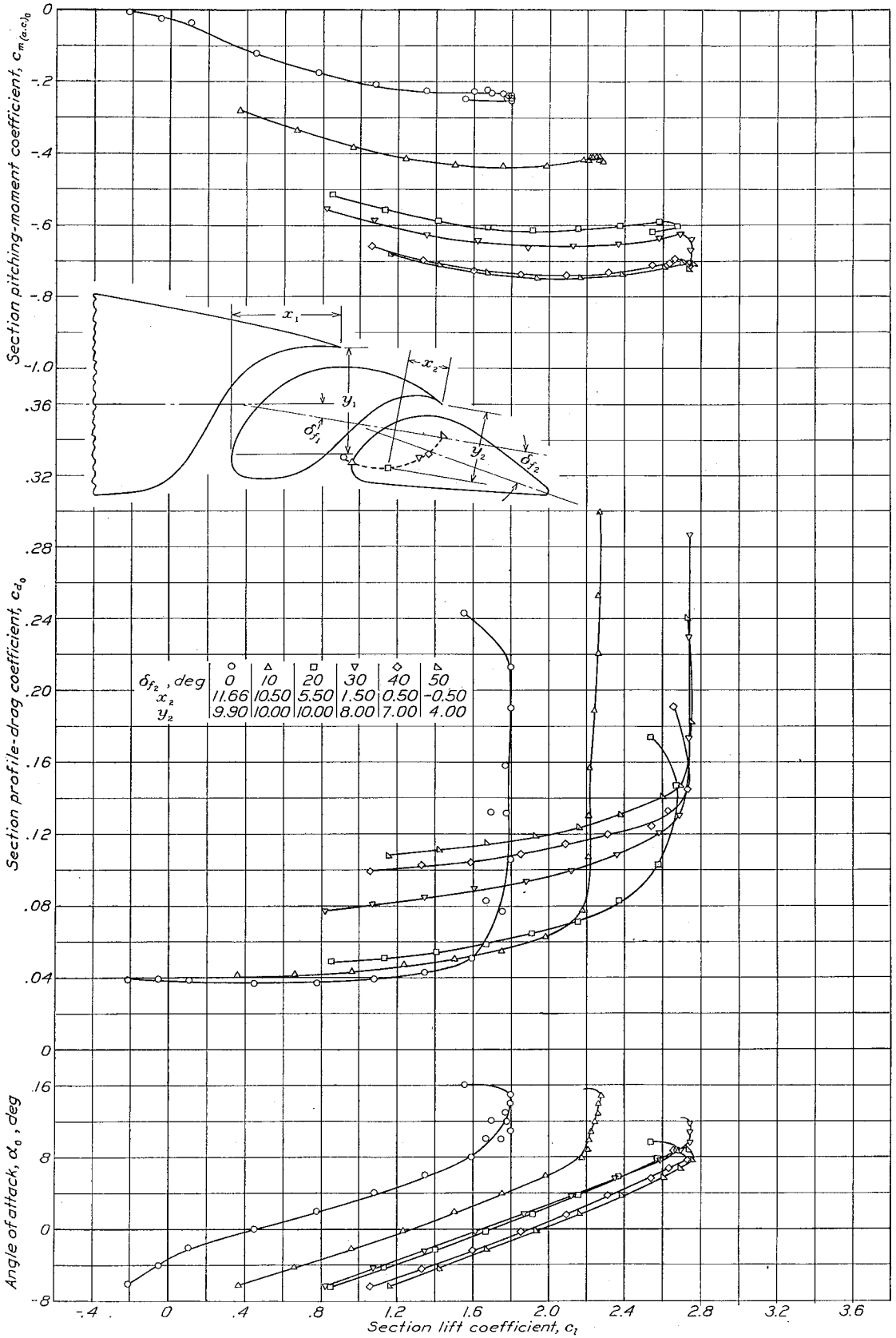

FIGURE 17.—Aerodynamic section characteristics of NACA 23030 airfoil with 40-percent-chord double slotted flap. $\delta_{f_1}=10°$; $x_1=14.50$; $y_1=15.00$. x_1, y_1, x_2, y_2 are given in percent airfoil chord.

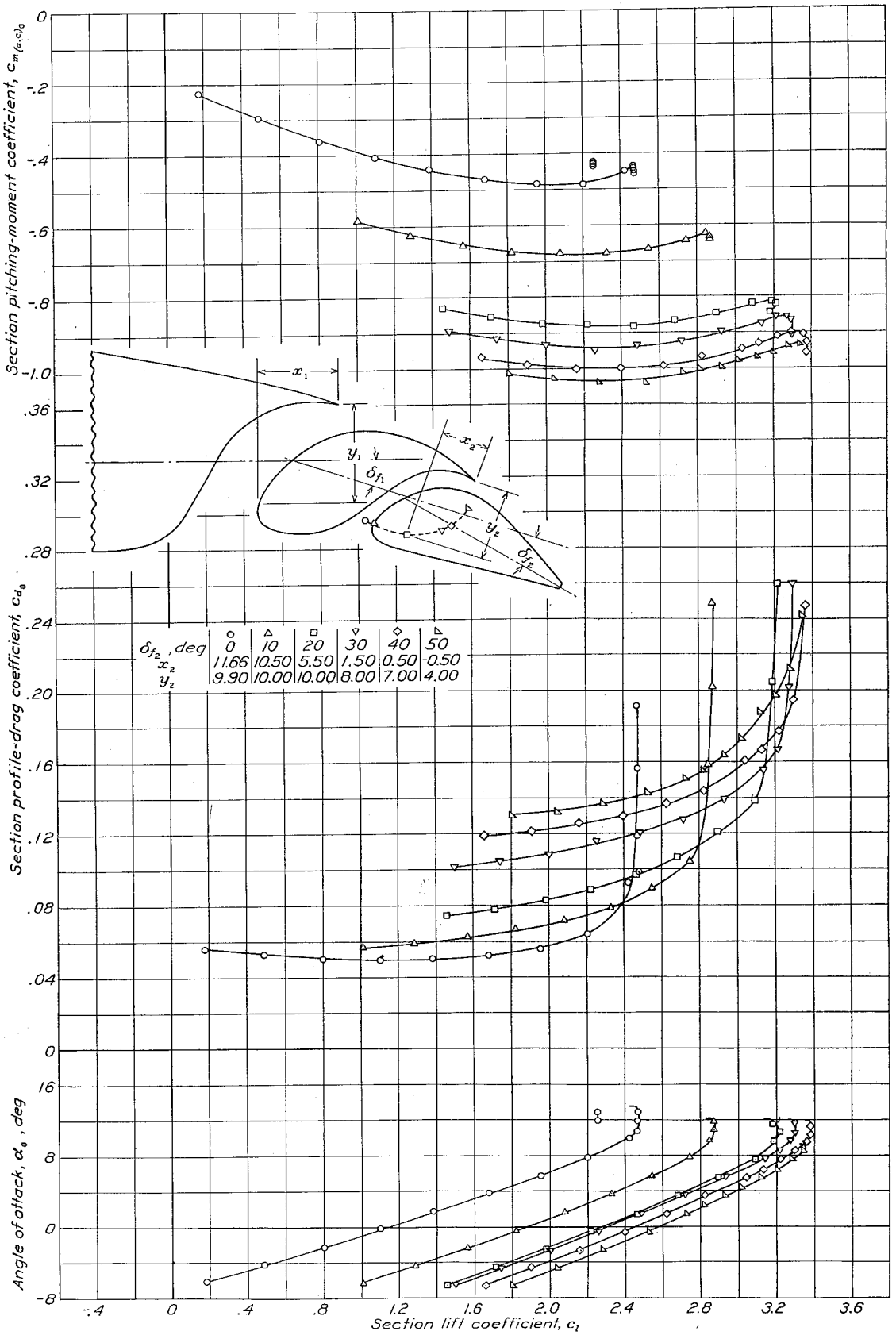

FIGURE 18.—Aerodynamic section characteristics of NACA 23030 airfoil with 40-percent-chord double slotted flap. $\delta_{f_1}=20°$; $x_1=10.50$; $y_1=14.00$. x_1, y_1, x_2, y_2 are given in percent airfoil chord.

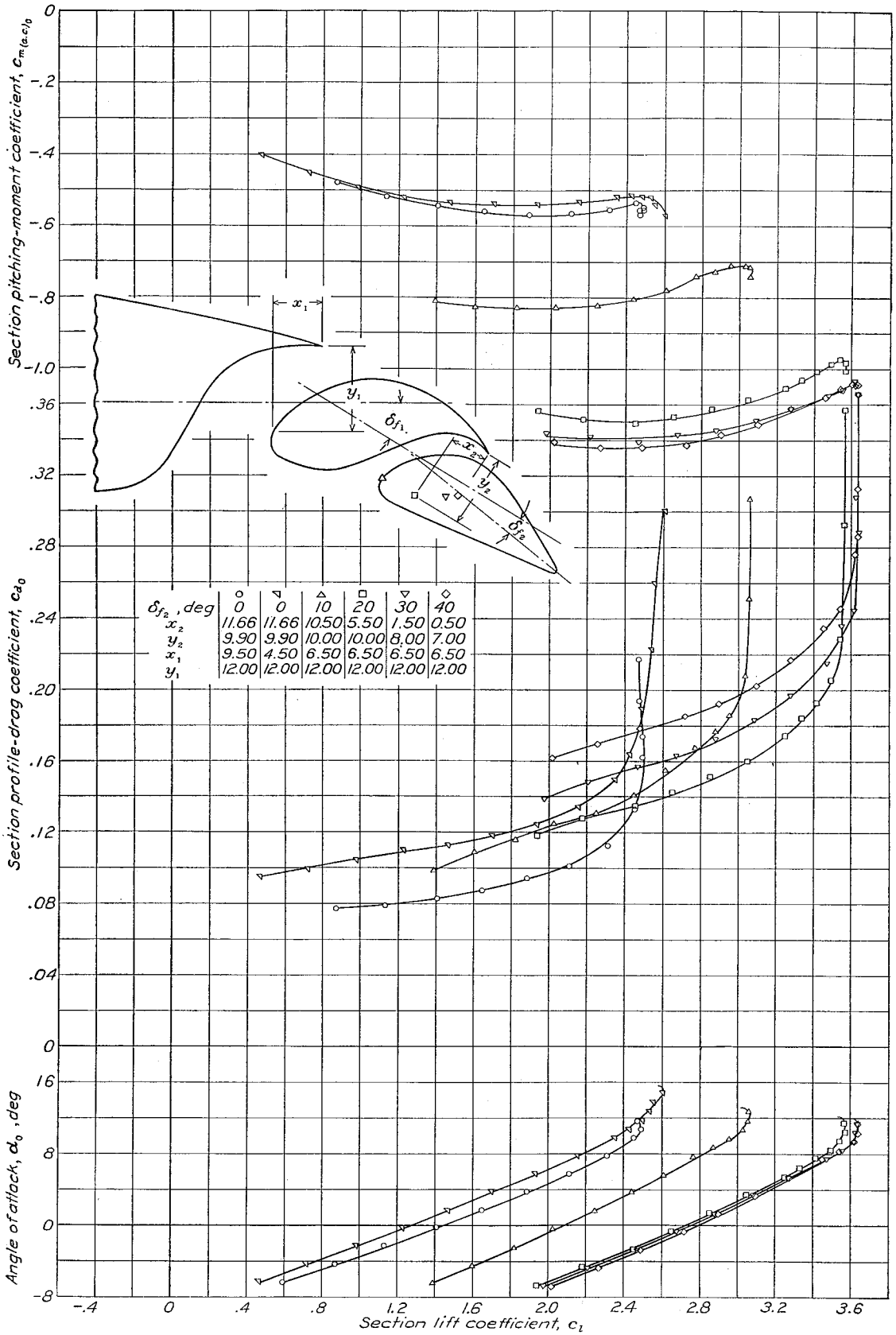

δ_{f_2}, deg	○ 0	▽ 0	△ 10	□ 20	▽ 30	◇ 40
x_2	11.66	11.66	10.50	5.50	1.50	0.50
y_2	9.90	9.90	10.00	10.00	8.00	7.00
x_1	9.50	4.50	6.50	6.50	6.50	6.50
y_1	12.00	12.00	12.00	12.00	12.00	12.00

FIGURE 19.—Aerodynamic section characteristics of NACA 23030 airfoil with 40-percent-chord double slotted flap. $\delta_{f_1}=30°$. x_1, y_1, x_2, y_2 are given in percent airfoil chord.

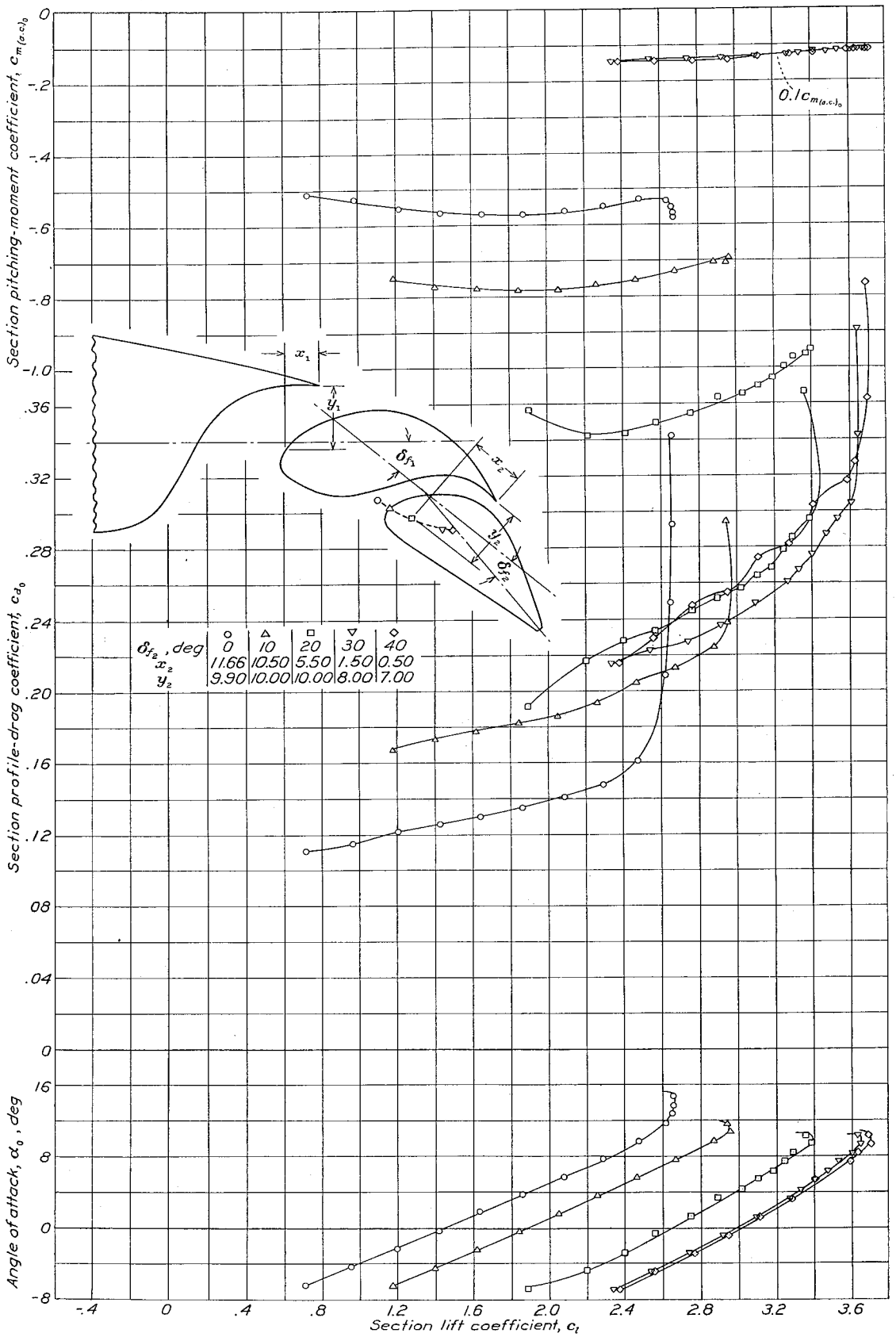

FIGURE 20.—Aerodynamic section characteristics of NACA 23030 airfoil with 40-percent-chord double slotted flap. $\delta_{f_1}=40°$; $x_1=4.50$; $y_1=9.00$. x_1, y_1, x_2, y_2 are given in percent airfoil chord.

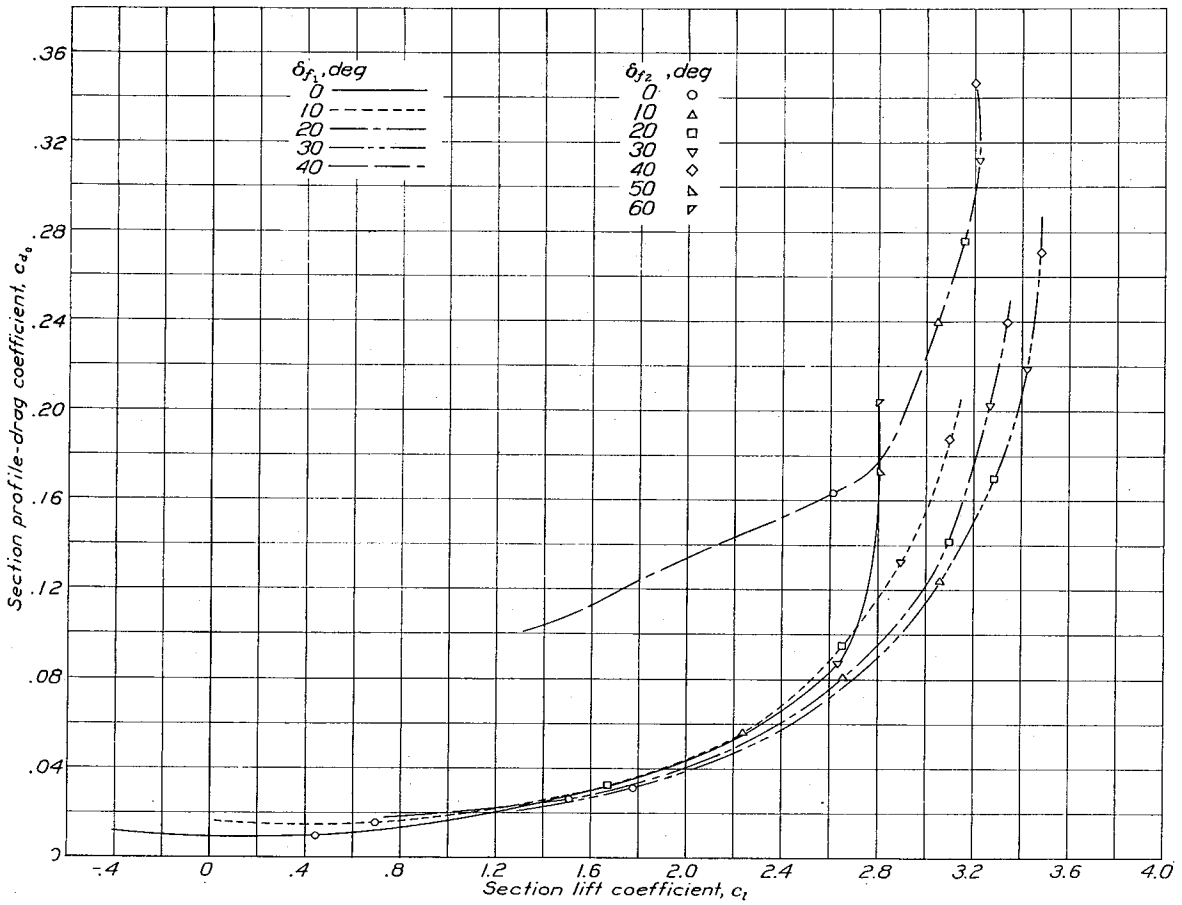

FIGURE 21.—Envelope polar curves for NACA 23012 airfoil with 40-percent-chord double slotted flap.

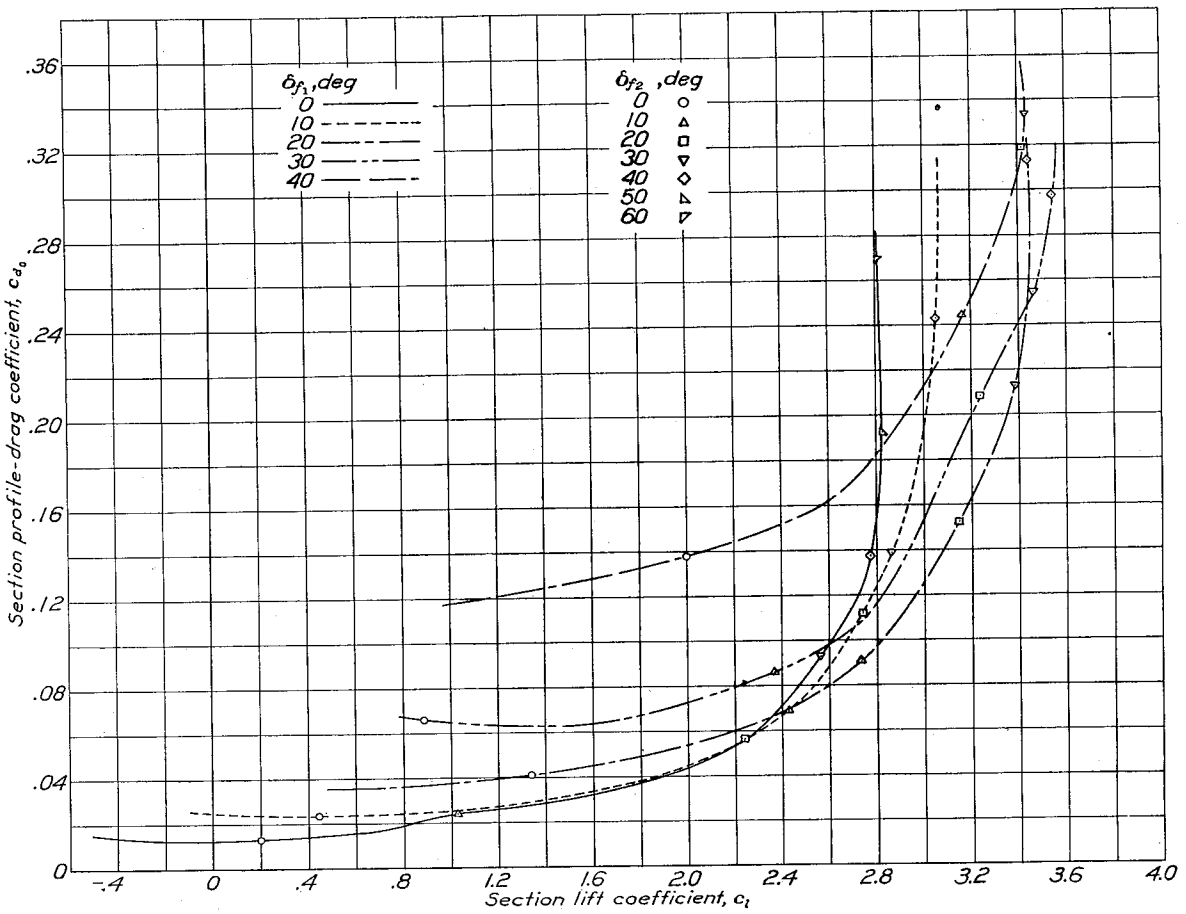

FIGURE 22.—Envelope polar curves for NACA 23021 airfoil with 40-percent-chord double slotted flap.

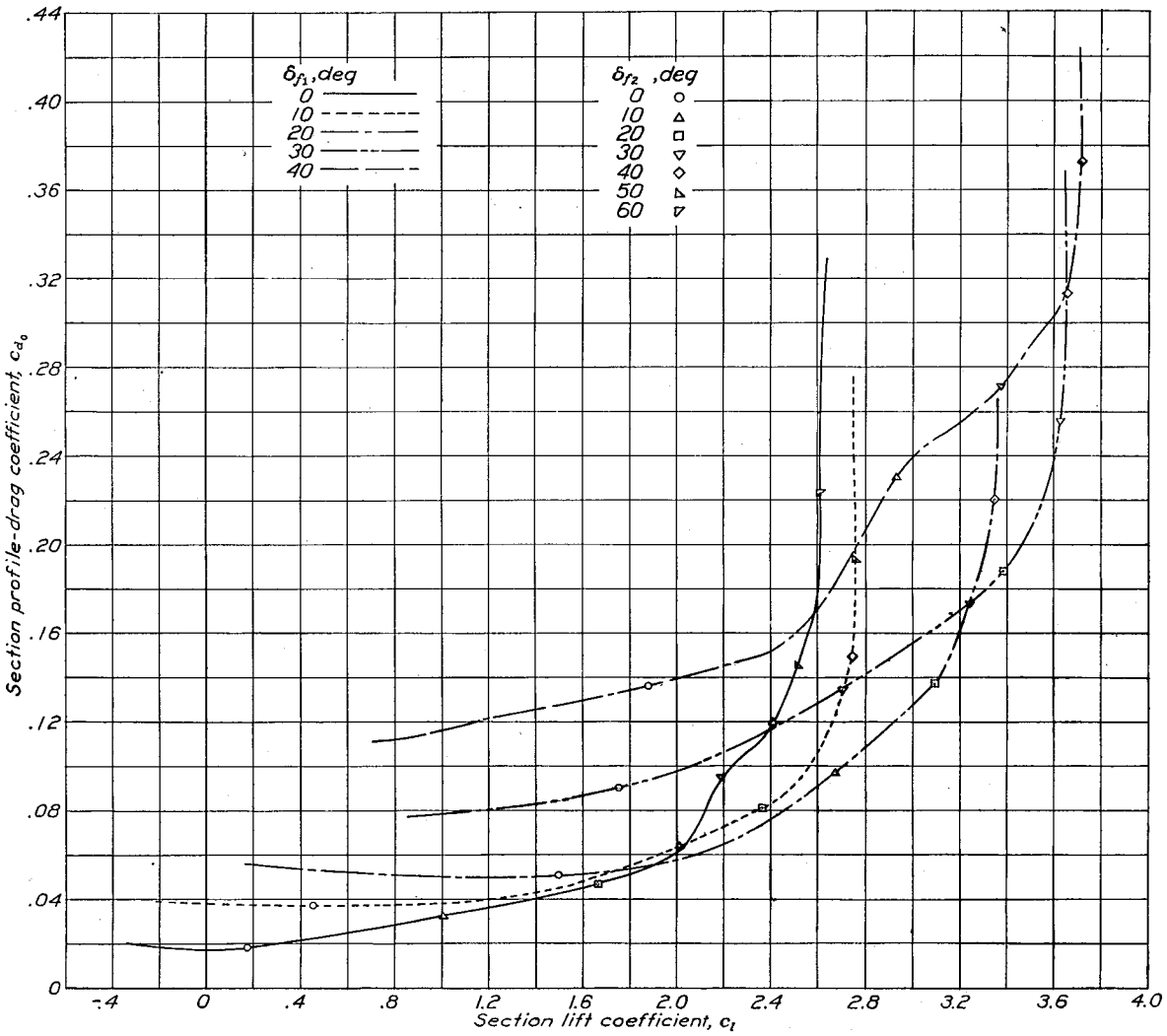

FIGURE 23.—Envelope polar curves for NACA 23030 airfoil with 40-percent-chord double slotted flap.

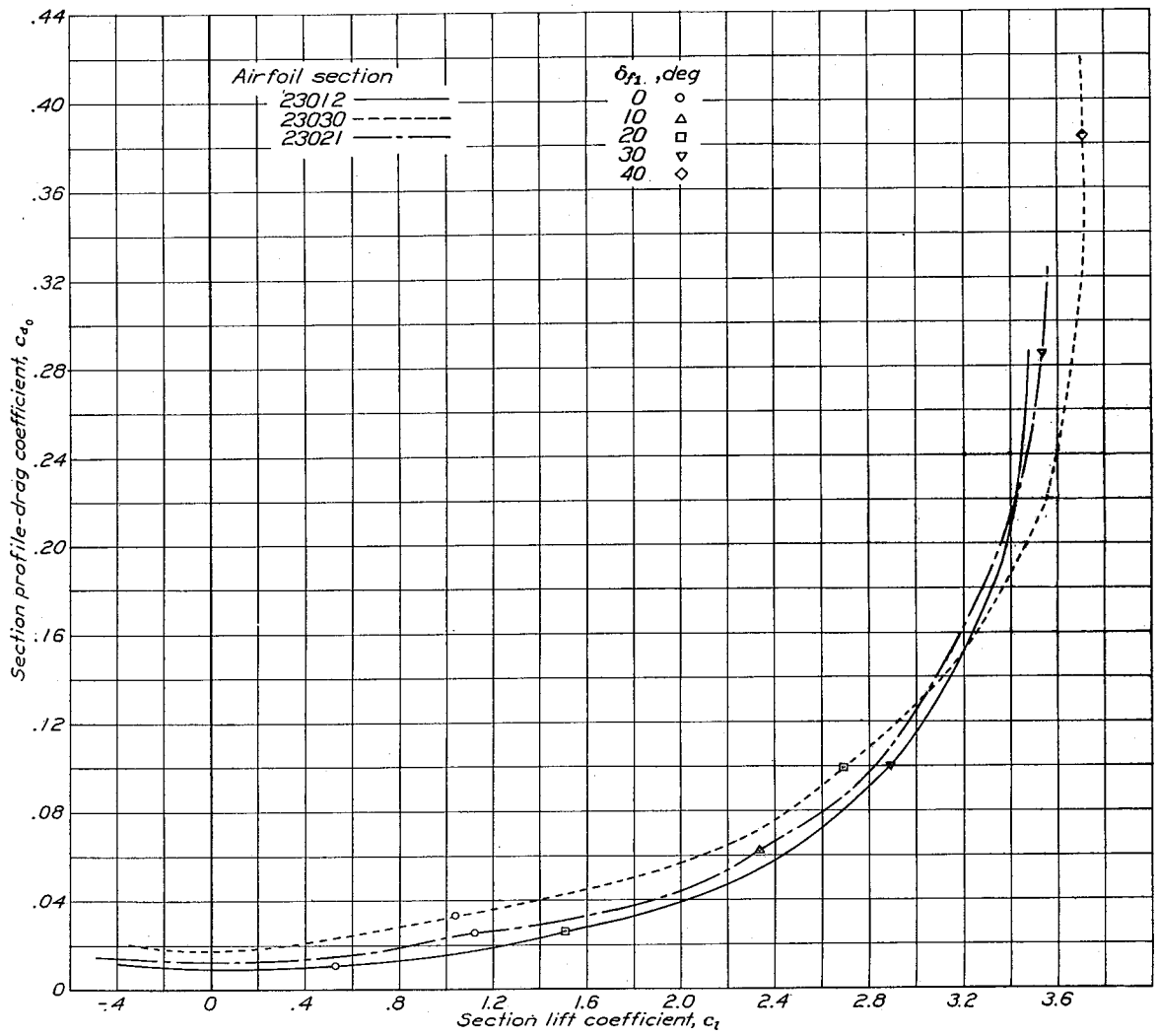

FIGURE 24.—Comparison of 40-percent-chord double slotted flap on NACA 23012, 23021, and 23030 airfoils.

The polar envelopes for the NACA 23021 airfoil (fig. 22) show that the plain wing gives the lowest value of section profile-drag coefficient for section lift coefficients less than 1.0. From $c_l=1.0$ to about $c_l=2.4$, the lowest section profile-drag coefficient is given by a main flap deflection of 0°; whereas, for section lift coefficients above 2.4, the minimum section profile-drag coefficient is given by $\delta_{f_1}=20°$. The section maximum lift coefficient is given by $\delta_{f_1}=30°$.

As in the case of the other two airfoils, the plain NACA 23030 airfoil (fig. 23) gives the lowest section profile-drag coefficient at low section lift coefficients. From $c_l=0.5$ to $c_l=1.9$, the section minimum profile-drag coefficients are obtained with a main flap deflection of 0°. In the lift range of 1.9 to 3.2, a 20° main flap deflection is required for optimum section profile-drag conditions, while a main flap deflection of 30° gives the lowest section profile-drag coefficients at section lift coefficients above 3.2. Maximum section lift is obtained with $\delta_{f_1}=40°$.

COMPARISON OF AIRFOILS OF DIFFERENT THICKNESS WITH DOUBLE SLOTTED FLAPS

Effect of thickness on profile drag.—Envelopes of the envelope polar curves of figures 21 to 23 are given in figure 24. These envelopes show the minimum section profile-drag coefficient that may be obtained with the three airfoils at any section lift coefficient. As has been previously noted, the profile-drag data for the NACA 23012 airfoil with $\delta_{f_1}=30°$ and $\delta_{f_2}=0°$ were erratic; the values of c_{d_0} over the lift range of $c_l=1.4$ to $c_l=1.9$ have been disregarded in drawing the envelope of the envelopes. The section profile-drag coefficient increases with the airfoil thickness throughout the lift range except above a section lift coefficient of about 3.2, where the 30-percent thick airfoil gives a lower section profile-drag coefficient than the others.

Effect of thickness on maximum lift.—The effect of the auxiliary flap deflection on the increment of section maximum lift coefficient with various main flap deflections is shown in figure 25 for the three airfoils. The increment of the section maximum lift increases not only with the auxiliary and the main flap deflections but also with the airfoil thickness. The maximum increment of section maximum lift coefficient $\Delta c_{l_{max}}$ is obtained with the NACA 23012 and 23030 airfoils when $\delta_{f_2}=40°$; the NACA 23021 airfoil gives the maximum $\Delta c_{l_{max}}$ when $\delta_{f_2}=30°$.

The effect of the main flap deflection on the increment

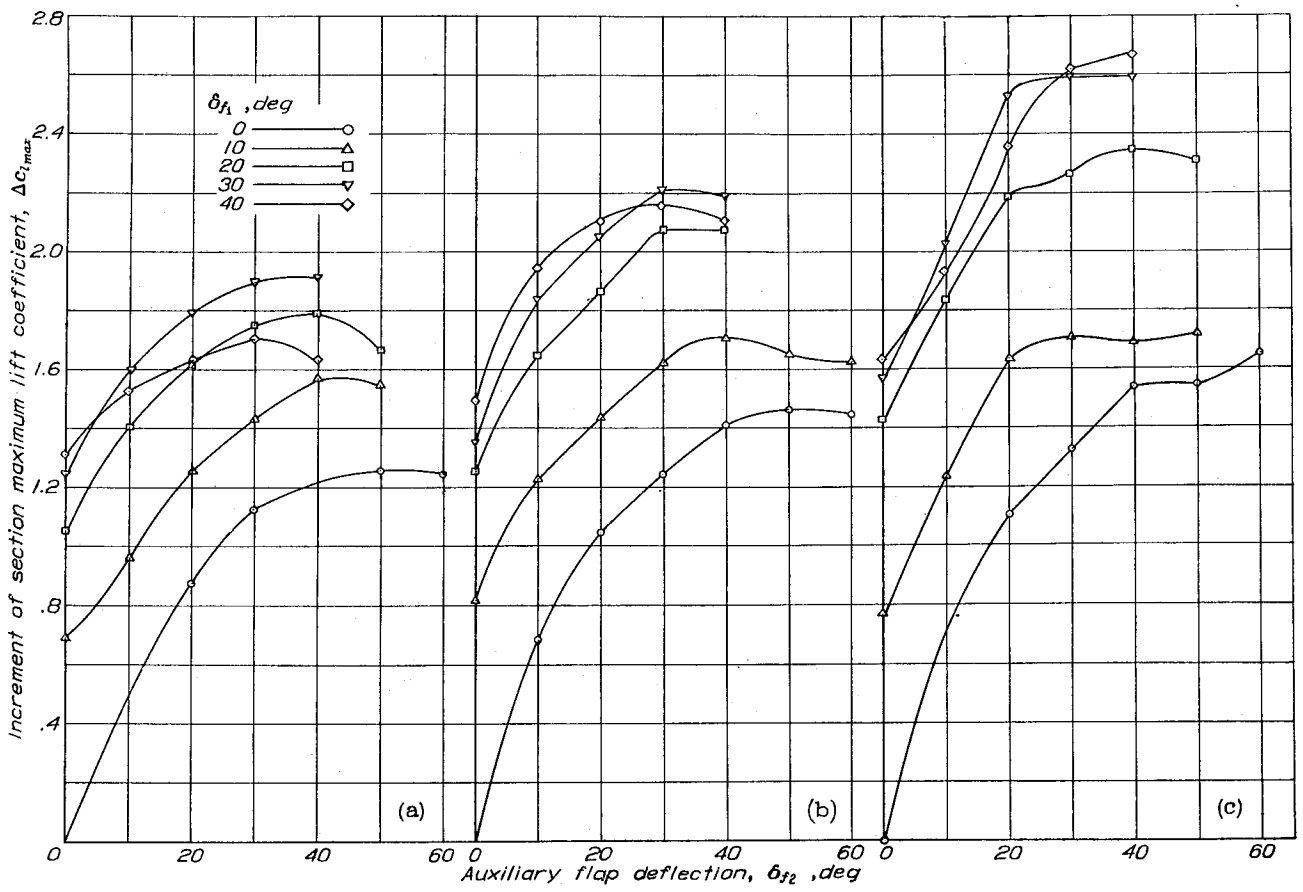

(a) NACA 23012 airfoil. (b) NACA 23021 airfoil. (c) NACA 23030 airfoil.

FIGURE 25.—Effect of auxiliary flap deflection on the increment of section maximum lift coefficient for the various airfoils.

of section maximum lift coefficient is shown in figure 26. The highest $\Delta c_{l_{max}}$ for the NACA 23012 and 23021 airfoils was given by a main flap deflection of 30° and, for the NACA 23030 airfoil, by a deflection of 40°. The maximum increments increase with airfoil thickness, and this effect becomes more marked as δ_{f_1} is increased. The rapid increase in the increment of the section maximum lift coefficient with airfoil thickness

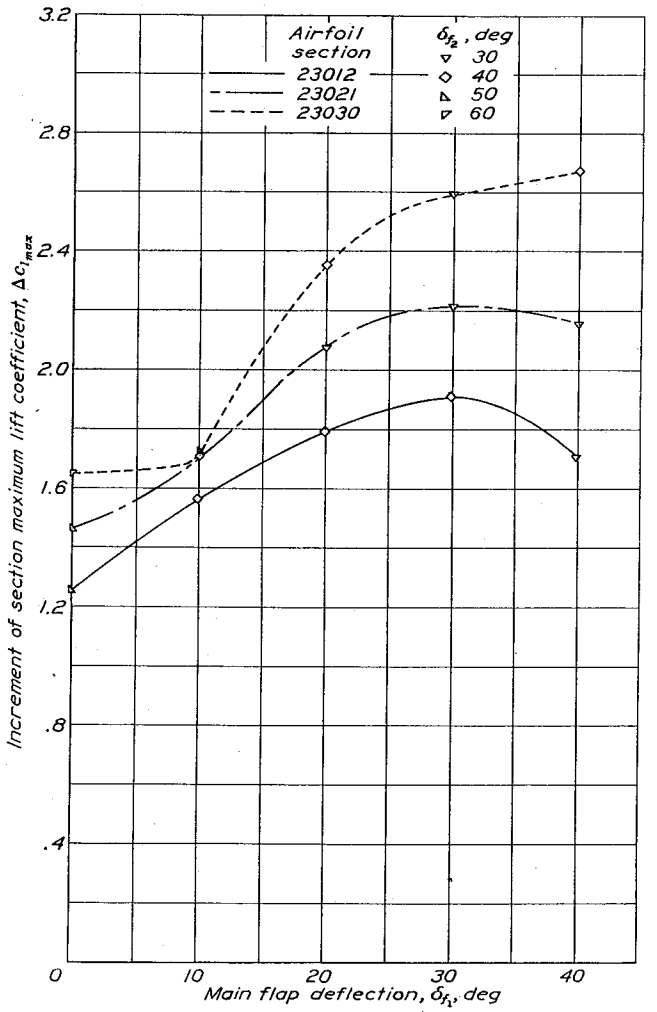

FIGURE 26.—Effect of main flap deflection on increment of section maximum lift coefficient of NACA 230 airfoils with 40-percent-chord double slotted flaps.

is not readily apparent in the final section maximum lift coefficient, which (as can be seen from fig. 27) is not greatly affected by thickness; and, whereas values of $\Delta c_{l_{max}}$ increase about 40 percent with an increase in airfoil thickness from 12 to 30 percent, the section maximum lift coefficient increases by only about 7 percent over the same thickness range. In view of the fact, however, that the section maximum lift coefficient of the plain airfoils decreases 30 percent with the increase in thickness, the small magnitude of the increase in maximum lift for the flapped airfoils is expected. It is of interest to note that similar results have been obtained with split flaps (reference 7) and single slotted flaps (reference 3).

COMPARISON OF VARIOUS SLOTTED FLAPS ON EACH AIRFOIL

Comparisons of a 25.66-percent slotted flap, a 40 percent slotted flap, and a 40-percent double slotted flap

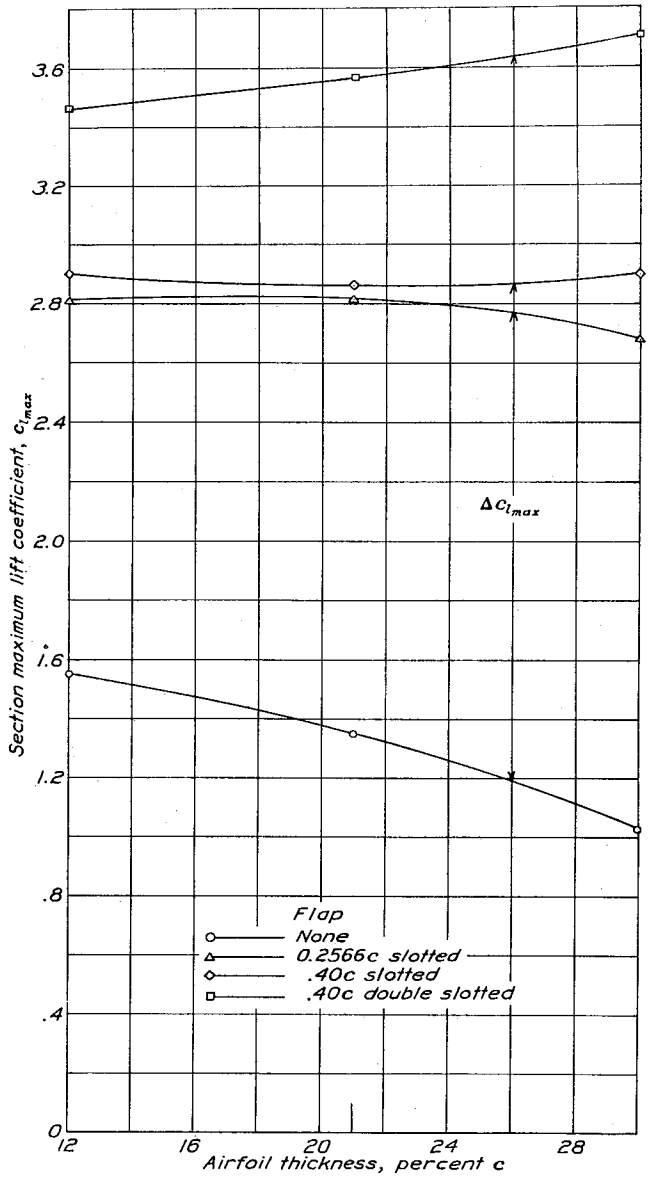

FIGURE 27.—Effect of airfoil thickness on section maximum lift coefficient of NACA 230 airfoils with and without slotted flaps.

on the NACA 23012, 23021, and 23030 airfoils are presented in figures 28, 29, and 30, respectively. At section lift coefficients below about 2.0, the double slotted flaps have about the same section profile-drag coefficients as the single slotted flaps for all three airfoils. For the higher section lift coefficients, the double slotted flaps give less section drag than the single slotted flaps.

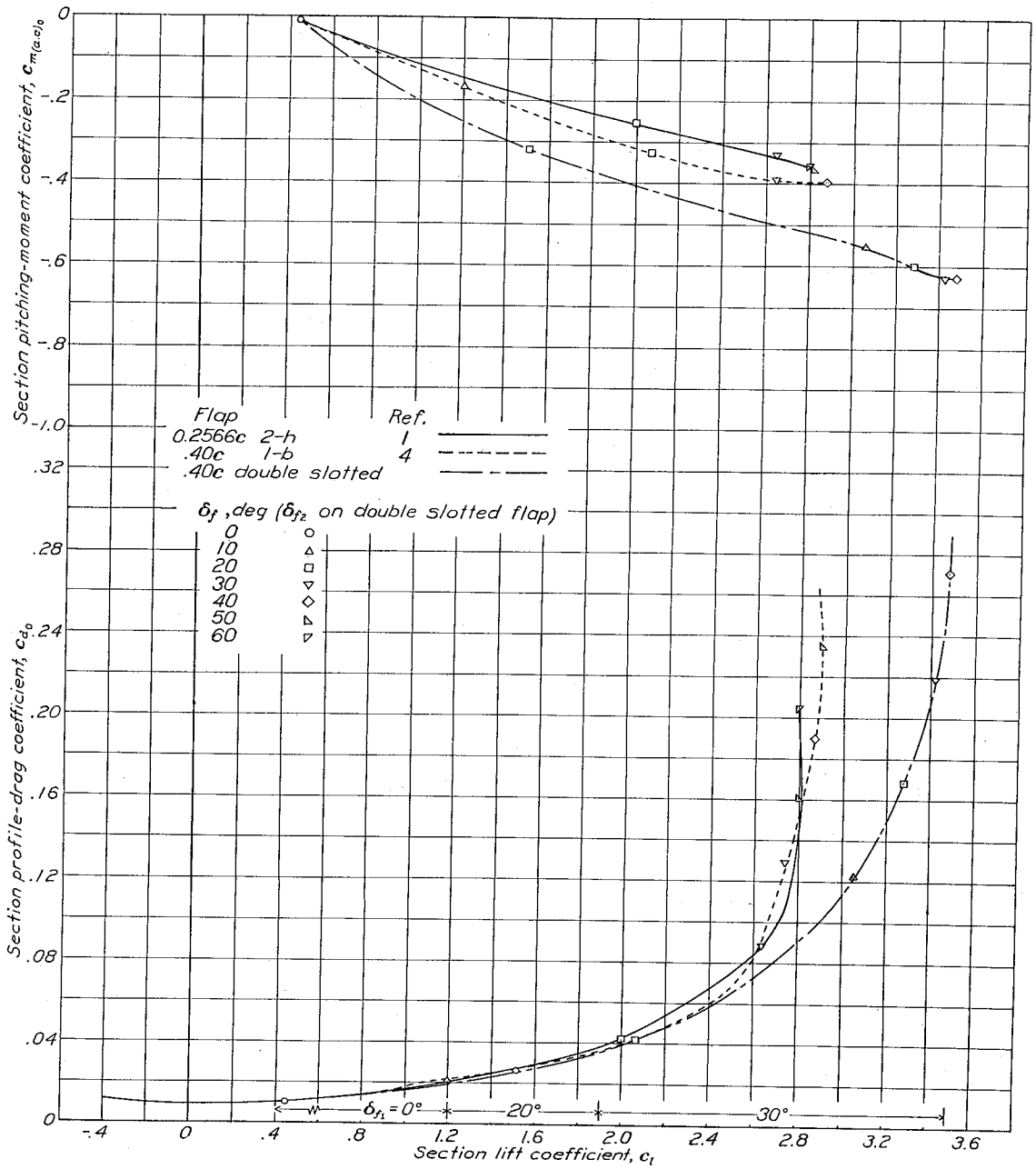

FIGURE 28.—Comparison of slotted flaps on NACA 23012 airfoil.

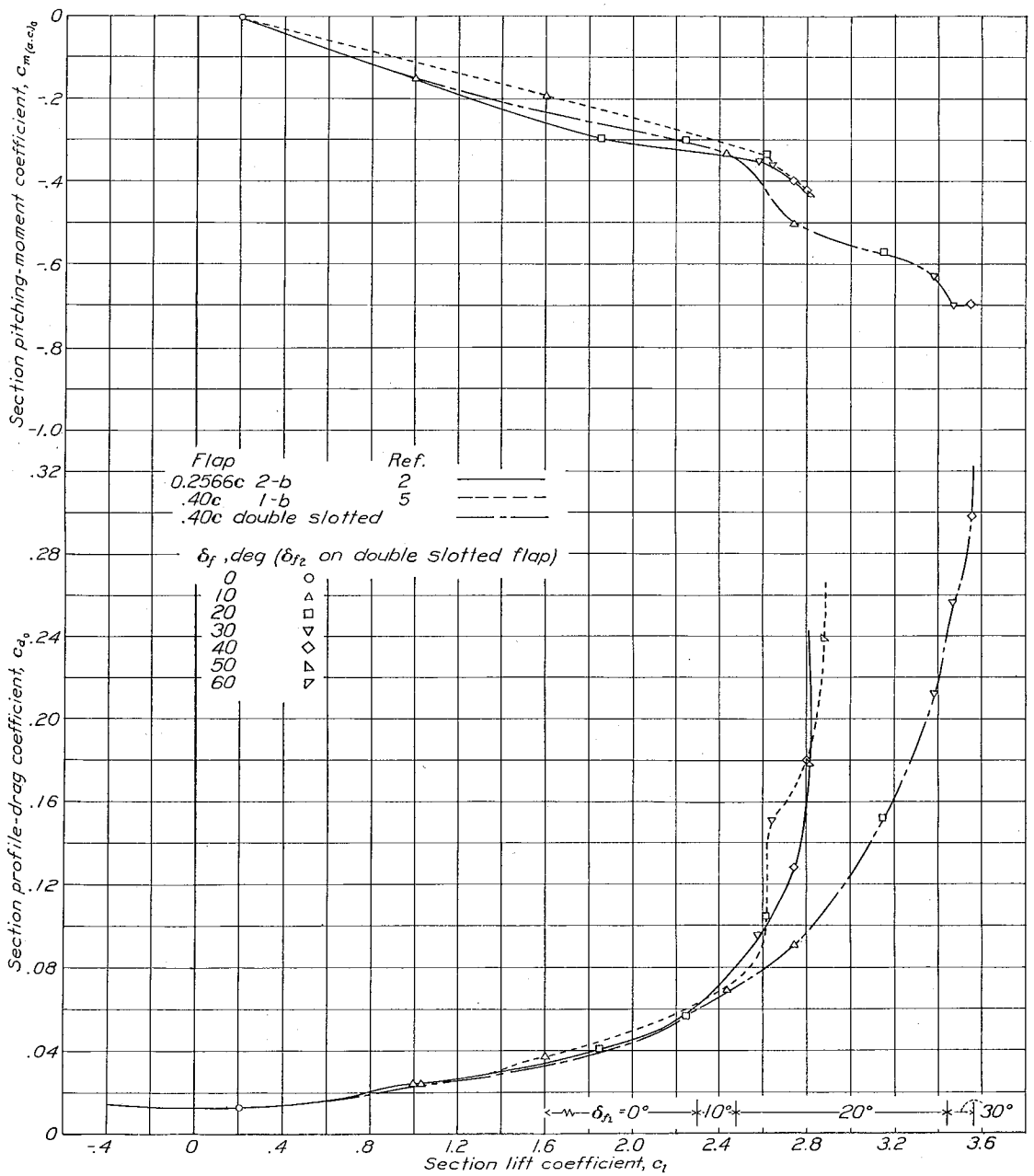

FIGURE 29.—Comparison of slotted flaps on NACA 23021 airfoil.

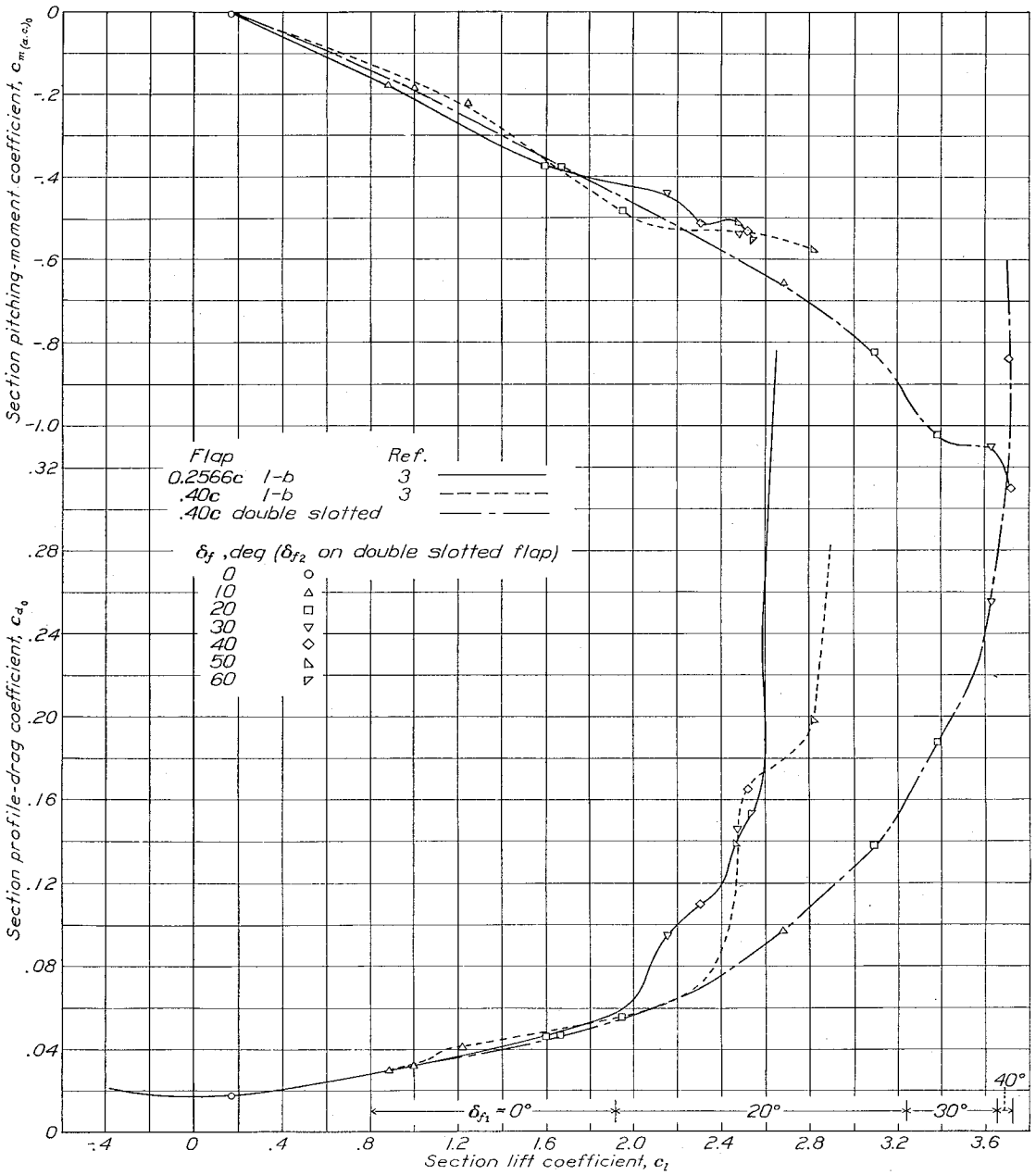

FIGURE 30.—Comparison of slotted flaps on NACA 23030 airfoil.

On the basis of the maximum obtainable section lift coefficient, the double slotted flaps show a considerable gain over the single slotted flaps on the airfoils (fig. 27). On the NACA 23012 airfoil, the increase in section maximum lift coefficient over that of the plain airfoil is 81 percent, 87 percent, and 123 percent for the 25.66-percent slotted flap, the 40-percent slotted flap, and the 40-percent double slotted flap, respectively. In the case of the NACA 23021 airfoil, the respective increases are 107 percent, 110 percent, and 162 percent;

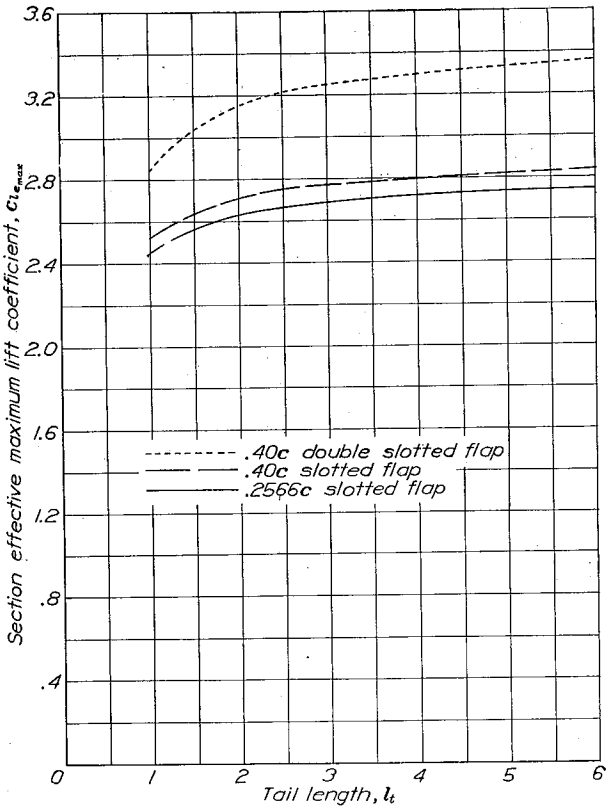

FIGURE 31.—Section effective maximum lift coefficients for slotted flaps on NACA 23012 airfoil.

while the increases for the NACA 23030 airfoil are 160 percent, 182 percent, and 260 percent.

Although the section maximum lift coefficients obtained with the double slotted flaps are greater than the coefficients obtained with either of the single slotted flaps regardless of airfoil thickness, it must be remembered that the pitching-moment coefficients are also greater. Thus, a double-slotted-flap installation will require a greater negative tail load to balance the pitching moment than will a single-slotted-flap installation, and it therefore appears desirable to take the tail load into consideration when the maximum lift coefficients are compared. Accordingly, section effective maximum lift coefficients were computed for each airfoil-flap combination for various tail lengths by the formula—

$$c_{l_{e_{max}}} = c_{l_{max}} + \frac{\left[c_{m_{(a.c.)_0}}\right] c_{l_{max}}}{l_t}$$

These data are presented in figures 31, 32, and 33. For

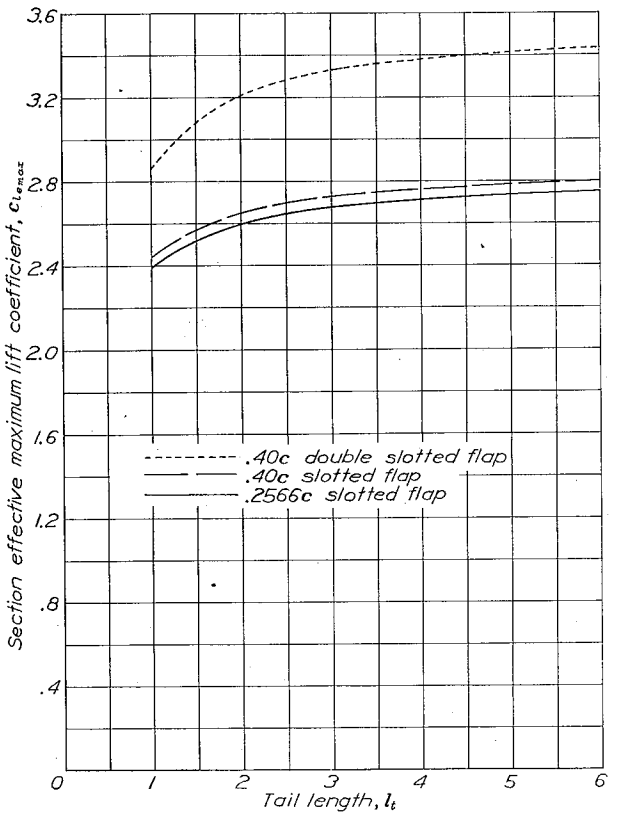

FIGURE 32.—Section effective maximum lift coefficients for slotted flaps on NACA 23021 airfoil.

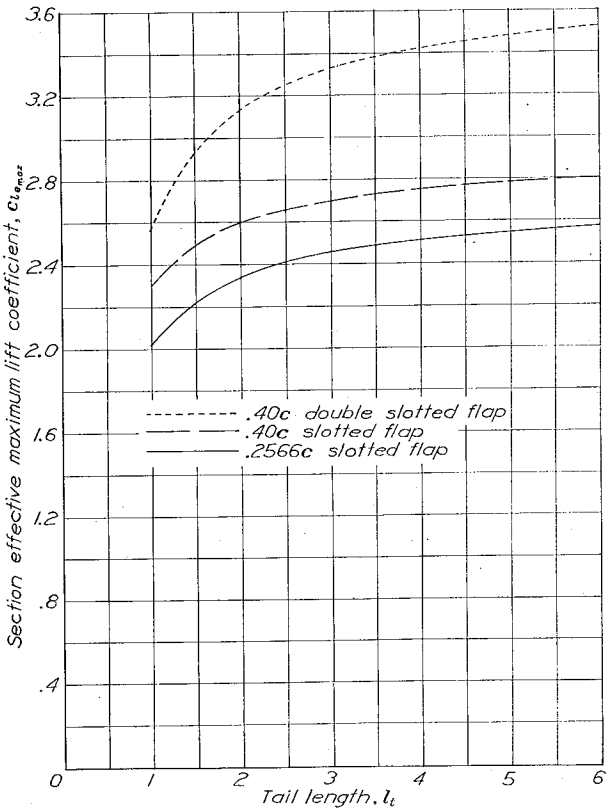

FIGURE 33.—Section effective maximum lift coefficients for slotted flaps on NACA 23030 airfoil.

each of the airfoils, the effective maximum lift coefficient obtained with the double slotted flap is greater than the coefficient obtained with either of the single slotted flaps. The superiority of the double slotted flaps in this respect increases with tail length.

The pitching-moment coefficients plotted in figures 28 to 30 are those obtained when the flaps are moved and deflected to the positions that give minimum values of section profile-drag coefficient at a given section lift coefficient. The difference in pitching-moment coefficients of the various slotted flaps is most marked for the NACA 23012 airfoil. On that airfoil the 25.66-percent-chord single slotted flap gives the lowest values of pitching-moment coefficient while the double slotted flap gives the highest values throughout the lift range. On the NACA 23021 airfoil the lowest values of pitching-moment coefficient are given by the 40-percent-chord single slotted flap while the 25.66-percent single slotted flap and the double slotted flap give about the same pitching-moment coefficients below $c_l=1.2$. In the case of the NACA 23030 airfoil there is little difference in the pitching-moment coefficients given by the three flaps for lift coefficients up to 1.6. For lift coefficients less than 1.6, the 40-percent single slotted flap gave the lowest pitching-moment coefficients while, at higher lift coefficients, the 25.66-percent single slotted flap gives the lowest value of pitching-moment coefficient.

CONCLUDING REMARKS

The effect of increasing the airfoil thickness on the aerodynamic characteristics of airfoils with double slotted flaps was to increase the section profile drag through most of the lift range although, at very high section lift coefficients, the section profile drag was reduced by an increasing thickness. The section maximum lift coefficient increased slowly with increasing airfoil thickness.

For a given airfoil thickness, the section profile drag of the 40-percent-chord single slotted flap, the 25.66-percent-chord single slotted flap, and the 40-percent-chord double slotted flaps was about the same at section lift coefficients less than 2.0. For higher section lift coefficients, the double slotted flap gave the lowest section profile-drag coefficient regardless of airfoil thickness. The section maximum lift coefficients of the airfoils with double slotted flaps were considerably higher than those of the airfoils with single slotted flaps for all airfoil thicknesses. The large lift coefficients for the double slotted flaps were accompanied by large pitching-moment coefficients.

LANGLEY MEMORIAL AERONAUTICAL LABORATORY,
NATIONAL ADVISORY COMMITTEE FOR AERONAUTICS,
LANGLEY FIELD, VA., *August 6, 1940.*

REFERENCES

1. Wenzinger, Carl J., and Harris, Thomas A.: Wind-Tunnel Investigation of an N. A. C. A. 23012 Airfoil with Various Arrangements of Slotted Flaps. Rep. No. 664, NACA, 1939.
2. Wenzinger, Carl J. and Harris, Thomas A.: Wind-Tunnel Investigation of an N. A. C. A. 23021 Airfoil with Various Arrangements of Slotted Flaps. Rep. No. 677, NACA, 1939.
3. Recant, I. G.: Wind-Tunnel Investigation of an N. A. C. A. 23030 Airfoil with Various Arrangements of Slotted Flaps. T. N. No. 755, NACA, 1940.
4. Harris, Thomas A.: Wind-Tunnel Investigation of an N. A. C. A. 23012 Airfoil with Two Arrangements of a Wide-Chord Slotted Flap. T. N. No. 715, NACA, 1939.
5. Duschik, Frank: Wind-Tunnel Investigation of an N. A. C. A. 23021 Airfoil with Two Arrangements of a 40-Percent-Chord Slotted Flap. T. N. No. 728, NACA, 1939.
6. Wenzinger, Carl J., and Harris, Thomas A.: Preliminary Wind-Tunnel Investigation of an N. A. C. A. 23012 Airfoil with Various Arrangements of Venetian-Blind Flaps. Rep. No. 689, NACA, 1940.
7. Wenzinger, Carl J., and Harris, Thomas A.: Wind-Tunnel Investigation of N. A. C. A. 23012, 23021, and 23030 Airfoils with Various Sizes of Split Flap. Rep. No. 668, NACA, 1939.
8. Wenzinger, Carl J., and Gauvain, William E.: Wind-Tunnel Investigation of an N. A. C. A. 23012 Airfoil with a Slotted Flap and Three Types of Auxiliary Flap. Rep. No. 679, NACA, 1939.
9. Harris, Thomas A.: The 7 by 10 Foot Wind Tunnel of the National Advisory Committee for Aeronautics. Rep. No. 412, NACA, 1931.
10. Jacobs, Eastman N., and Sherman, Albert: Airfoil Section Characteristics as Affected by Variations of the Reynolds Number. Rep. No. 586, NACA, 1937.

TABLE I

ORDINATES FOR NACA 230 AIRFOILS

[Stations and ordinates in percent of airfoil chord]

Station	NACA 23012		NACA 23021		NACA 23030	
	Upper surface	Lower surface	Upper surface	Lower surface	Upper surface	Lower surface
0	-------	0	-------	0	4.82	0
1.25	2.67	−1.23	4.87	−2.08	7.37	−2.63
2.5	3.61	−1.71	6.14	−3.14	8.90	−4.27
5	4.91	−2.26	7.93	−4.52	11.05	−6.54
7.5	5.80	−2.61	9.13	−5.55	12.57	−8.28
10	6.43	−2.92	10.03	−6.32	13.68	−9.65
15	7.19	−3.50	11.19	−7.51	15.20	−11.52
20	7.50	−3.97	11.80	−8.30	16.07	−12.61
25	7.60	−4.28	12.05	−8.76	16.46	−13.20
30	7.55	−4.46	12.06	−8.95	16.57	−13.46
40	7.14	−4.48	11.49	−8.83	15.89	−13.13
50	6.41	−4.17	10.40	−8.14	14.38	−12.11
60	5.47	−3.67	8.90	−7.07	12.34	−10.47
70	4.36	−3.00	7.09	−5.72	9.86	−8.42
80	3.08	−2.16	5.05	−4.13	7.03	−6.09
90	1.68	−1.23	2.76	−2.30	3.87	−3.40
95	.92	−.70	1.53	−1.30	2.15	−1.86
100	.13	−.13	.22	−.22	.32	−.32
L. E. radius	1.58		4.85		9.90	

Slope of radius through end of chord: 0.305

TABLE II
ORDINATES FOR FLAPS ON NACA 230 AIRFOILS

[Stations and ordinates in percent of airfoil chord]

Station	NACA 23012 airfoil				NACA 23021 airfoil			
	Main flap		Auxiliary flap		Main flap		Auxiliary flap	
	Upper surface	Lower surface	Upper surface	Lower surface	Upper surface	Lower surface	Upper surface	Lower surface
0	−1.76	−1.76	−1.29	−1.29	−2.70	−2.70	−0.55	−0.55
.32							.59	−1.81
.40			−.32	−2.05				
.63	−.31				0			
.64							1.08	−2.30
.72			.04	−2.21				
1.25	.37	−3.17			1.00			
1.28							1.89	−2.88
1.36			.61	−2.36				
1.93							2.44	−3.28
2.00			1.04	−2.41				
2.50	1.36	−3.40			2.48			
2.57							2.88	−3.53
2.64			1.40	−2.41				
3.92			1.94					
5.00	2.69	−3.36			4.51	−6.14		
5.14							3.96	−3.91
5.20			2.30					
5.66				−2.16				
6.48			2.53					
7.50	3.48	−3.19			5.85	−6.09		
7.70							4.26	−3.79
7.76			2.63					
9.03			2.58					
10.00	3.97	−3.00			6.59	−5.72		
10.27							3.99	−3.34
10.31			2.46					
11.00	4.05				6.70			
12.00	4.07							
12.83							3.42	−2.84
15.40							2.83	−2.36
15.66			1.68	−1.23				
17.96							2.21	−1.86
20.00	3.08	−2.16			5.05	−4.13		
20.53							1.56	−1.35
20.66			.92	−.70				
23.10							.90	−.81
25.66			.13	−.13			.22	−.22
30.00	1.68	−1.23			2.76	−2.30		
35.00	.92	−.70			1.53	−1.30		
40.00	.13	−.13			.22	−.22		
	Center of L. E. arc							
	1.35	−1.76	0.91	−1.29	3.78	−2.15	2.89	−0.55
L. E. radius	1.35		0.91		3.80		2.89	

U. S. GOVERNMENT PRINTING OFFICE: 1942

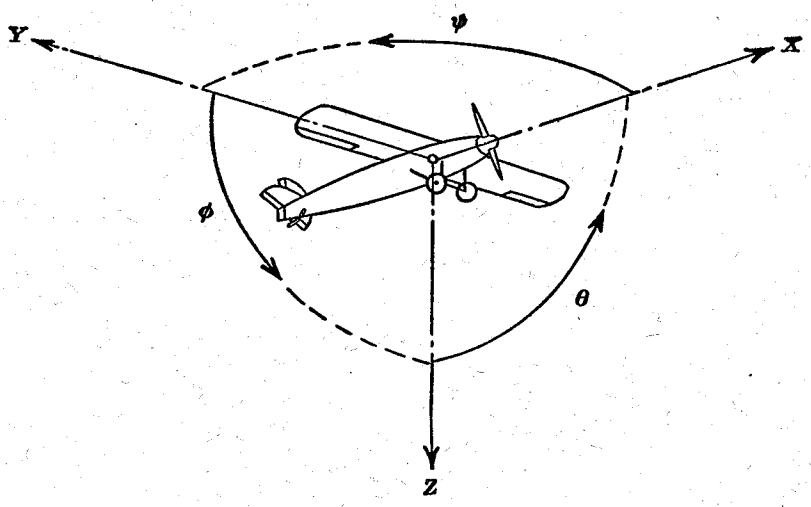

Positive directions of axes and angles (forces and moments) are shown by arrows

Axis		Force (parallel to axis) symbol	Moment about axis			Angle		Velocities	
Designation	Symbol		Designation	Symbol	Positive direction	Designation	Symbol	Linear (component along axis)	Angular
Longitudinal	X	X	Rolling	L	$Y \longrightarrow Z$	Roll	ϕ	u	p
Lateral	Y	Y	Pitching	M	$Z \longrightarrow X$	Pitch	θ	v	q
Normal	Z	Z	Yawing	N	$X \longrightarrow Y$	Yaw	ψ	w	r

Absolute coefficients of moment

$C_l = \frac{L}{qbS}$ (rolling) $\quad C_m = \frac{M}{qcS}$ (pitching) $\quad C_n = \frac{N}{qbS}$ (yawing)

Angle of set of control surface (relative to neutral position), δ. (Indicate surface by proper subscript.)

4. PROPELLER SYMBOLS

D, Diameter

p, Geometric pitch

p/D, Pitch ratio

V', Inflow velocity

V_s, Slipstream velocity

T, Thrust, absolute coefficient $C_T = \frac{T}{\rho n^2 D^4}$

Q, Torque, absolute coefficient $C_Q = \frac{Q}{\rho n^2 D^5}$

P, Power, absolute coefficient $C_P = \frac{P}{\rho n^3 D^5}$

C_s, Speed-power coefficient $= \sqrt[5]{\frac{\rho V^5}{P n^2}}$

η, Efficiency

n, Revolutions per second, r.p.s.

Φ, Effective helix angle $= \tan^{-1}\left(\frac{V}{2\pi r n}\right)$

5. NUMERICAL RELATIONS

1 hp.=76.04 kg-m/s=550 ft-lb./sec.
1 metric horsepower=1.0132 hp.
1 m.p.h.=0.4470 m.p.s.
1 m.p.s.=2.2369 m.p.h.

1 lb.=0.4536 kg.
1 kg=2.2046 lb.
1 mi.=1,609.35 m=5,280 ft.
1 m=3.2808 ft.